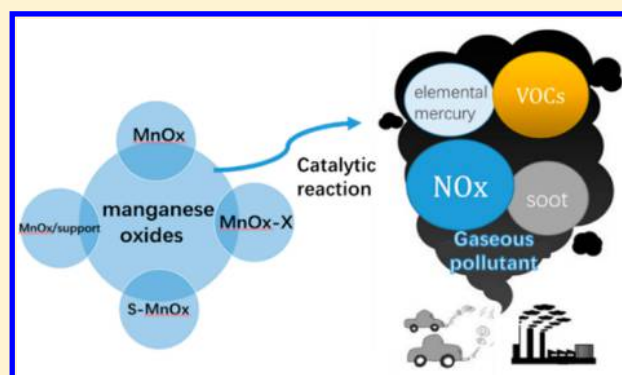


# Gaseous Heterogeneous Catalytic Reactions over Mn-Based Oxides for Environmental Applications: A Critical Review

Haomiao Xu, Naiqiang Yan,\*<sup>ORCID</sup> Zan Qu, Wei Liu, Jian Mei, Wenjun Huang, and Songjian Zhao

School of Environmental Science and Engineering, Shanghai Jiao Tong University, 800 Dongchuan RD, Minhang District, Shanghai, China

**ABSTRACT:** Manganese oxide has been recognized as one of the most promising gaseous heterogeneous catalysts due to its low cost, environmental friendliness, and high catalytic oxidation performance. Mn-based oxides can be classified into four types: (1) single manganese oxide (MnOx), (2) supported manganese oxide (MnOx/support), (3) composite manganese oxides (MnOx-X), and (4) special crystalline manganese oxides (S-MnOx). These Mn-based oxides have been widely used as catalysts for the elimination of gaseous pollutants. This review aims to describe the environmental applications of these manganese oxides and provide perspectives. It gives detailed descriptions of environmental applications of the selective catalytic reduction of NOx with NH<sub>3</sub>, the catalytic combustion of volatile organic compounds, Hg<sup>0</sup> oxidation and adsorption, and soot oxidation, in addition to some other environmental applications. Furthermore, this review mainly focuses on the effects of structure, morphology, and modified elements and on the role of catalyst supports in gaseous heterogeneous catalytic reactions. Finally, future research directions for developing manganese oxide catalysts are proposed.



## 1. INTRODUCTION

Manganese, a transition metal element, and its oxides widely exist in the environment. Manganese oxides, assembled from the basic structure of [MnO<sub>6</sub>] units, can form various types of Mn-based oxides.<sup>1,2</sup> These Mn-based oxides possess a number of superior physical and chemical properties, such as high reversible capacitance, structural flexibility and stability, fast cation diffusion under high charge–discharge rates, and environmental friendliness.<sup>3,4</sup>

Mn-based oxides hold great promise for broad applications as electrode materials,<sup>3,5,6</sup> sorbents,<sup>7,8</sup> and catalysts<sup>9,10</sup> mainly due to their high redox potential, environmental friendliness, and low cost. Furthermore, Mn-based materials often have high structure flexibility, and they can be modified by catalyst supports and other elements. The application of Mn-based oxides for gaseous heterogeneous catalytic reactions was first exhibited decades ago.<sup>11</sup> The materials exhibited high heterogeneous catalytic performance. Currently, Mn-based oxides are often used as catalysts for the selective catalytic reduction (SCR) of NOx with NH<sub>3</sub>, the catalytic combustion of volatile organic compounds (VOCs), Hg<sup>0</sup> oxidation and adsorption, soot oxidation, CO oxidation, etc.<sup>12–15</sup> In these reactions, it was found that the high catalytic performance relies on the type of Mn-based catalyst used. According to the literature,<sup>3,9,10</sup> numerous Mn-based oxides have been developed using various synthetic methods. Simply, they can be classified into four types: (1) single manganese oxide (MnOx), (2) supported manganese oxide (MnOx/support), (3) composite manganese oxide (MnOx-X), and (4) special crystalline

manganese oxide (S-MnOx). A great deal of work has been done to investigate the catalytic performance of manganese oxides. However, there are still no reports summarizing these manganese oxide catalysts in gaseous heterogeneous catalytic reactions for environmental applications.

This review summarizes different types of Mn-based metal oxides. We focus on providing more basic information on the effects of the crystal structure, morphology, catalyst support, etc. of manganese oxides on the gaseous heterogeneous catalytic reactions. This review can benefit the design and synthesis of novel manganese oxide catalysts.

## 2. TYPES OF MN-BASED OXIDES

**2.1. Single Manganese Oxide (MnOx).** Single manganese oxide (MnOx) can exist as a variety of stable oxides, such as MnO,<sup>16</sup> Mn<sub>3</sub>O<sub>4</sub>,<sup>17</sup> Mn<sub>2</sub>O<sub>3</sub>,<sup>17,18</sup> MnO<sub>2</sub>,<sup>19</sup> etc. These Mn-based oxides present different crystal structures, morphologies, porosities, and textures, which are associated with a variety of properties. The structural parameters play a crucial role in the catalytic oxidation performance. Investigation of the influence of these characteristics of Mn-based oxides is the basis for the rational design of improved Mn-based oxides.

Received: December 20, 2016

Revised: June 19, 2017

Accepted: June 29, 2017

Published: June 29, 2017

Extensive effort has been dedicated to adjust the synthetic conditions to obtain manganese oxides with desirable morphologies, defect chemistries (cation distributions and oxidation states), and crystal structures to improve the catalytic performance. Although manganese oxides exist as many types of crystal structures, the structural frameworks consist of  $[\text{MnO}_6]$  octahedra sharing vertices and edges. The stacking of the  $[\text{MnO}_6]$  octahedra enables the construction of one-dimensional (1D),<sup>19,20</sup> two-dimensional (2D),<sup>21</sup> or three-dimensional (3D) tunnel structures.<sup>22</sup> For instance,  $\text{MnO}_2$  exhibits  $\alpha$ -,  $\beta$ -,  $\gamma$ -,  $\delta$ -,  $\epsilon$ -, and  $\lambda$ - $\text{MnO}_2$  structures under different synthetic conditions.  $\alpha$ -,  $\beta$ -, and  $\gamma$ - $\text{MnO}_2$  have 1D chain molecular structures,<sup>23,24</sup>  $\delta$ - $\text{MnO}_2$  has a 2D planar structure, and  $\lambda$ - $\text{MnO}_2$  has a 3D structure.<sup>3,25</sup> In addition, these manganese oxides can exhibit urchin-like, rod-like, flower-like, etc. morphologies under different synthetic conditions.<sup>26–28</sup>

As gaseous heterogeneous catalysts, manganese oxides with different crystal structures or morphologies exhibit considerable differences in catalytic performance. It has been shown that the catalytic performance of different MnOx depends strongly on the crystalline structure.<sup>29</sup>  $\alpha$ -,  $\beta$ -, and  $\gamma$ -MnOx synthesized using different methods often have different catalytic performances for the removal of gaseous pollutants.<sup>30,31</sup> In general, a higher valence of Mn was favorable for catalytic oxidation.  $\text{MnO}_2$  usually has a higher catalytic oxidation performance than  $\text{Mn}_2\text{O}_3$  or  $\text{MnO}$ . Furthermore, different morphologies of MnOx also lead to different catalytic performances.<sup>26</sup> Recent studies have developed novel synthetic methods to change the morphology and enhance the catalytic performance. Investigation of the catalytic performance of single MnOx can benefit the further modification of manganese oxides. In addition, it is better to investigate the reaction mechanism, the effect of crystal structure, and the effect of morphology features over such pure MnOx.

## 2.2. Supported Manganese Oxide (MnOx/Support).

Supported manganese oxide (MnOx/support) is a common catalyst for heterogeneous catalytic reactions. MnOx is the primary active site, and the support can enhance the performance of MnOx. Activated carbon (AC),<sup>32</sup> carbon nanotubes (CNTs),<sup>6,33</sup> Ce–Zr solid solutions,<sup>34</sup>  $\text{Al}_2\text{O}_3$ ,<sup>35</sup> etc. are often selected as catalyst supports for MnOx particles. The usual roles of these supports are as follows: First, the support enlarges the surface area for MnOx active sites. The catalyst support provides a very large surface area over which the active sites are dispersed, preventing particle aggregation. Additionally, the catalyst support can provide room for the catalytic reaction to occur. For example, AC and CNTs are often used as catalyst supports to supply space for the active sites and the catalytic reaction. Second, the supports enhance the catalytic performance of MnOx. Some catalyst supports are beneficial for improving the properties of the system and participate in the reaction. For example, graphene can enhance the electron transfer performance of MnOx during catalytic reaction.<sup>30</sup>  $\text{CeO}_2$  can enhance the  $\text{O}_2$  storage performance, which is beneficial for gaseous pollutants adsorption and catalytic oxidation.

According to the literature, the various catalyst supports can be classified as carbon-based supports and noncarbon-based supports. AC, CNTs, graphene, carbon spheres, and fly ash are often used as carbon-based supports.<sup>32,36</sup> These carbon-based materials usually have large surface areas. It is well-known that the carbon family includes carbon spheres (0D), CNTs (1D), graphene (2D), porous carbon and amorphous carbon

(3D).<sup>37,38</sup> Carbon spheres supported MnOx can obtain a large specific surface area, uniform pore-size distribution, and excellent capacitance performance.<sup>39</sup> CNTs are a type of representative nanostructured carbon material and exhibit outstanding physicochemical properties such as high electrical conductivity, mechanical strength, chemical stability, and large surface areas.<sup>5,33,40</sup> The combination of MnOx and CNTs can take advantage of both the excellent properties of CNTs and the specific catalytic performance of MnOx. The incorporation of  $\text{MnO}_2$  on a CNT support can be realized through chemical coprecipitation, thermal decomposition, and electrophoretic and electrochemical deposition methods.<sup>3</sup> As a novel material in the carbon family, graphene exhibits unique properties due to its 2D structure.<sup>37,41</sup> It supplies sufficient space for catalytic reaction and can prevent MnOx particle agglomeration.<sup>30</sup> However, the MnOx/graphene composite still needs to be improved for real applications as a catalyst. Using porous carbon and AC as catalyst supports for MnOx was first shown decades ago. The 3D structure is beneficial for the adsorption of gaseous pollutants.

Noncarbon supports, such as  $\text{Al}_2\text{O}_3$ ,<sup>42,43</sup>  $\text{CeO}_2$ ,<sup>44</sup> Ce–Zr solid solutions,<sup>34</sup> etc., have been used for MnOx. These catalytic supports can be classified into two types. The first does not take part in the catalytic reaction, such as  $\text{Al}_2\text{O}_3$  and zeolites.<sup>9</sup> These catalyst supports only play the role of supplying space for the catalytic reaction or dispersing MnOx particles. The second type of catalyst supports, such as  $\text{CeO}_2$  and Ce–Zr solid solutions, often work as adsorption sites for the reaction.  $\text{CeO}_2$  has been shown to have high  $\text{O}_2$  storage capacity, which is beneficial for catalytic oxidation. Ce–Zr solid solutions can further enhance the  $\text{O}_2$  storage performance, and it is the most used noncarbon catalytic support for various catalytic reactions. Although there existed many types of catalyst supports, the basic function was the high dispersion of Mn active sites. Furthermore, developing novel catalyst supports is essential to enhance the magnetic properties, thermal properties, electrical properties, and mechanical properties of the system.

## 2.3. Composite Manganese Oxides (MnOx-X).

Composite metal oxide (MnOx-X) catalysts are of great interest due to their modifying effects on manganese oxides, which can enhance the thermodynamic stability, electronic properties, and surface properties. These modifying elements can be classified as (1) noble metal elements, (2) transition metal elements, (3) main group elements, and (4) rare earth elements.

Noble metal or metal oxides such as  $\text{RuO}_2$ ,<sup>45</sup> Ir,<sup>46</sup> Ag,<sup>47</sup> etc., usually show catalytic performances. However, the high price of noble metal limits its wide usage. With the addition of manganese oxides, the cost decreased. The interaction between noble metals and MnOx can enhance the catalytic performance of the system. For example, Xu et al. prepared an Ag– $\text{MnO}_2$  composite for the catalytic oxidation of CO.<sup>31</sup> The results indicated that a strong interaction occurred between Ag and  $\text{MnO}_2$ . The catalytic activity clearly correlates with this interaction, which is determined by the crystal phase and surface structure. Most transition metal oxides, such as  $\text{Fe}_2\text{O}_3$ ,<sup>48</sup>  $\text{CuO}$ ,<sup>49</sup>  $\text{V}_2\text{O}_5$ ,<sup>50</sup>  $\text{CoOx}$ ,<sup>51</sup> etc., also show catalytic performance for gaseous pollutants to some extent. Composites of MnOx and these transition metal oxides could synergistically enhance the catalytic performance of the system. In general, MnOx often suffers from  $\text{SO}_2$  poisoning and low reactivity at high temperature.<sup>9,52</sup> With the addition of transition metal oxides, Fe–MnOx could protect MnOx from  $\text{SO}_2$  poisoning. In many

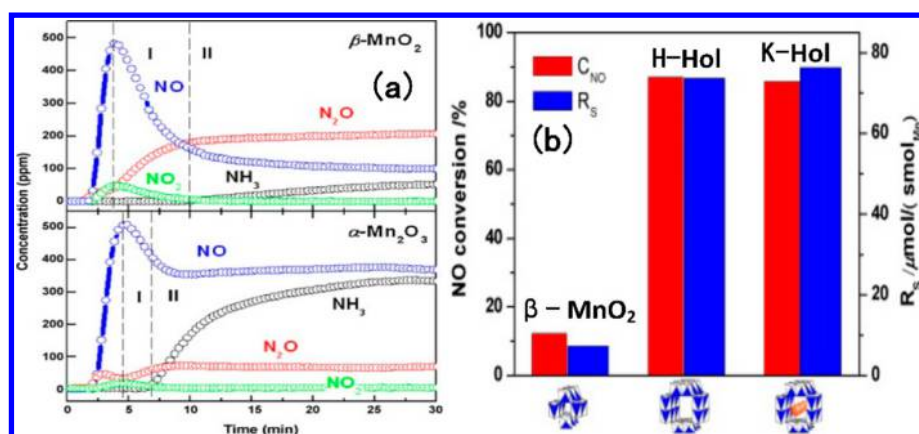


**Figure 1.** (a) Transition reactions of  $\text{NH}_3 + \text{NO}$  on the studied catalysts in the presence of  $\text{O}_2$ . Conditions: catalyst = 200 mg,  $\text{NO} = 680$  ppm,  $\text{NH}_3 = 680$  ppm,  $\text{O}_2 = 3.0\%$  with  $\text{N}_2$  balance, gas rate = 300 mL/min, temperature = 150 °C;<sup>76</sup> (b) NO conversions and special reaction rates of NO in the  $\text{NH}_3$ -SCR reactions over  $\beta\text{-MnO}_2$ , H-Hol, and K-Hol. Conditions:  $\text{NH}_3 = \text{NO} = 500$  ppm,  $\text{O}_2 = 3.0\%$  with  $\text{N}_2$  balance, gas rate = 1000 mL/min,  $\text{GHSV} = 110\,000\ \text{h}^{-1}$ .<sup>77</sup>

cases, MnOx has a higher catalytic performance at low temperature. Moreover, with the addition of FeOx or CoOx, the activity at high temperature can be enhanced.<sup>53,54</sup> Some main group elements, such as Zr and Sn, are commonly used for the modification of MnOx.<sup>55,56</sup> Both of these oxides have nearly no activity in catalytic reactions. However, the incorporation of main group elements into MnOx enhanced the properties of MnOx. SnO<sub>2</sub> can enlarge the reaction window due to the enhanced electron transfer performance of chemically adsorbed O<sub>2</sub>. In addition, SnO<sub>2</sub> can convert adsorbed O<sub>2</sub> to O<sup>2-</sup> at high temperature, which is favorable for catalytic reactions.<sup>57,58</sup> Similarly, a strong interaction exists between ZrO<sub>2</sub> and MnOx, such that the Zr-MnOx composite has a larger surface area and higher catalytic performance than pure MnOx.<sup>59</sup> Rare earth elements are often used for the modification of MnOx. Ce is used most often, and Ce-MnOx composites have exhibited excellent performances in many catalytic reactions.<sup>44,60–62</sup> CeO<sub>2</sub> has excellent oxygen storage performance and can capture gaseous O<sub>2</sub> from flue gas. Oxygen adsorbed on the surface could offer suitable adsorption sites for gaseous pollutants. Recently, ternary composite oxides or multicomposite oxides have been developed to further enhance the performance of MnOx. Understanding the role of each element and the interaction of these elements is beneficial for designing a catalyst for application under certain conditions. In addition, using composite manganese oxides should concentrate on enhancing the performance of sulfur resistance, water resistance, and high temperature resistance.

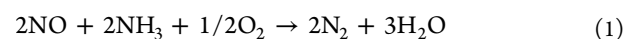
**2.4. Special Crystalline MnOx (S-MnOx).** Recent studies have found that some special crystalline structures have significant effects on catalytic oxidation, especially perovskite oxides and spinel metal oxides. Perovskite oxides are widely used for many environmental applications. Perovskite, originating from CaTiO<sub>3</sub>, is the general name for oxides that have the structural formula ABO<sub>3</sub>.<sup>63–65</sup> In the ABO<sub>3</sub> structure, Mn can occupy the B site, and the A site cation can be an alkali metal element or rare earth element. The material has high structural stability, and the A and/or B site can be substituted by a foreign cation. Such modification can change the oxidation state or the oxygen vacancy, thus offering a route to enhance the catalytic performance of the catalyst. In addition, spinel manganese oxides also show some catalytic performance.<sup>66,67</sup> In its AB<sub>2</sub>O<sub>4</sub> structure, the A site is a bivalent cation, and the B site is a

trivalent cation. This structure also offers catalytic performance. However, it has been accepted that oxygen vacancies and surface oxygen promote the catalytic reaction. An imperfect structure of S-MnOx is reasonable for application. The modification of S-MnOx should consider the structural effect on the reaction. Now it still lacks the investigation of S-MnOx for various applications.

### 3. ENVIRONMENTAL APPLICATIONS

NO<sub>x</sub>, Hg<sup>0</sup>, soot, and VOCs are four primary gaseous pollutants in the atmosphere. They represent main emission pollutant, heavy metal pollutant, particle pollutant, and organic pollutant, respectively. In addition, these pollutants are controlled using different methods over Mn-based oxides materials. For example, NO<sub>x</sub> was reduced to N<sub>2</sub> through the  $\text{NH}_3$ -SCR method, Hg<sup>0</sup> was oxidized to soluble Hg<sup>2+</sup> due to high oxidation performance of MnOx or was adsorbed on MnOx's surface, soot elimination was an oxidation process, while VOCs removal was a catalytic combustion process. Herein, we review NO<sub>x</sub>, Hg<sup>0</sup>, soot and VOCs as target pollutants for environmental applications over Mn-based oxides.

**3.1. Selective Catalytic Reduction of NO<sub>x</sub> with NH<sub>3</sub>.** Nitrogen oxides (NO<sub>x</sub>) are major air pollutants in the atmosphere. They are primarily emitted from coal-fired power plants, industrial heaters, and cogeneration plants. The  $\text{NH}_3$ -selective catalytic reduction ( $\text{NH}_3$ -SCR) of NO<sub>x</sub> is considered to be an efficient method for reducing NO<sub>x</sub> emissions.<sup>68–70</sup> The reaction with ammonia is given by the equation:



In this reaction, a catalyst is crucial to promote the interaction of  $\text{NH}_3$ , NO, and O<sub>2</sub>. To date, various kinds of SCR catalysts have been developed for this  $\text{NH}_3$ -SCR reaction. Traditional commercial SCR catalysts, such as V-W-TiO<sub>2</sub>/V-Mo-TiO<sub>2</sub>, have been indicated to have high reaction activity.<sup>71,72</sup> Moreover, these catalysts are efficient at high operating temperatures (300–400 °C), which make it necessary to locate the SCR unit upstream of the electrostatic precipitator. Recently, studies put more effort into the low-temperature (<200 °C) de-NO<sub>x</sub> reaction. Among the low-temperature  $\text{NH}_3$ -SCR catalysts, MnO<sub>x</sub> is one of the most efficient materials.<sup>9,73,74</sup>

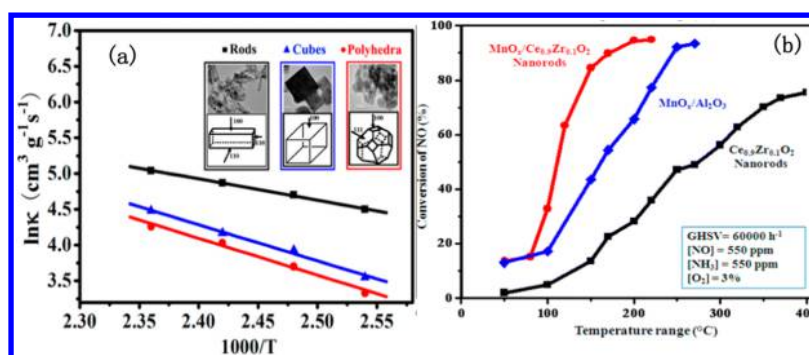


Figure 2. (a) Effect of the morphology of  $\text{ZrO}_2\text{-CeO}_2$  on the performance<sup>85</sup> and (b) the performance of a Ce-Zr solid solution.<sup>87</sup>

Kapteijn et al. investigated the  $\text{NH}_3\text{-SCR}$  performance of MnOx with different crystallinities.<sup>75</sup>  $\text{MnO}_2$  exhibited the highest activity per unit surface area, followed by  $\text{Mn}_5\text{O}_8$ ,  $\text{Mn}_2\text{O}_3$ ,  $\text{Mn}_3\text{O}_4$ , and MnO. In addition,  $\text{Mn}_2\text{O}_3$  is preferred in SCR since it has the highest selectivity toward nitrogen formation during this process. Furthermore, the selectivity decreases with increasing temperature. The oxidation state of manganese, the crystallinity, and the specific surface area are decisive factors in the performance of these oxides. Tang et al. investigated the  $\text{NH}_3\text{-SCR}$  performance over  $\beta\text{-MnO}_2$  and  $\alpha\text{-Mn}_2\text{O}_3$ ,<sup>76</sup> as shown in Figure 1a, and the activity evaluation showed that the rates of both NO conversion and  $\text{N}_2\text{O}$  formation per unit surface area on  $\beta\text{-MnO}_2$  were much higher than the corresponding values on  $\alpha\text{-Mn}_2\text{O}_3$ . Wang et al. studied hollandite-type manganese oxides with  $\text{K}^+$  or  $\text{H}^+$  cations in the tunnels (K-Hol or H-Hol).<sup>77</sup> As shown in Figure 1b, the results showed that both K-Hol and H-Hol had almost the same catalytic activities but much higher reaction rates than  $\beta\text{-MnO}_2$  under the same conditions.

Supported manganese oxides have been widely studied for low-temperature  $\text{NH}_3\text{-SCR}$  catalysis. Catalyst supports can enlarge the surface area for active sites and create room for the reaction to occur. These catalyst supports can be molecular sieves (such as zeolites,<sup>78,79</sup> ZSM-5,<sup>80-82</sup> SBA-15,<sup>83</sup> and SSZ-13<sup>84</sup>), Ce-Zr solid solutions,<sup>85-89</sup> metal oxides (such as V-based oxides,<sup>90,91</sup>  $\text{TiO}_2$ ,<sup>91-95</sup> and Ce- $\text{TiO}_2$ <sup>61</sup>), and carbon-based<sup>86,96-102</sup> materials.

Zeolite is a promising catalyst support. With the addition of zeolite, the thermal stability of MnOx can be enhanced. Young et al. synthesized a series of Fe-Mn metal oxides on a ZSM-5 support. The high dispersion  $\text{MnO}_2$  and high surface acidity of the catalyst were found to be responsible for the high de-NOx performance.<sup>82</sup> Molecular sieves offer a complex structure with microporous-mesoporous characteristics and specific surface properties that impart high thermal stability. SBA-15 is appropriate for use in the SCR of NO with  $\text{NH}_3$  due to its adjustable pore diameter, thick pore walls, and excellent hydrothermal stability.<sup>83</sup> Many metal oxides are commonly used as catalyst supports for manganese oxide.  $\text{TiO}_2$ -based supports are the most studied material for the  $\text{NH}_3\text{-SCR}$  reaction. Pure  $\text{TiO}_2$  has no activity in the  $\text{NH}_3\text{-SCR}$  reaction. However, MnOx can be well dispersed on its surface to allow MnOx to demonstrate its catalytic performance. Panagiotis et al. prepared a series of  $\text{TiO}_2$ -,  $\text{Al}_2\text{O}_3$ -, and  $\text{SiO}_2$ -supported manganese oxide catalysts for  $\text{NH}_3\text{-SCR}$ . The SCR performance of the supported Mn catalysts decreased in the following order:  $\text{TiO}_2$  (anatase, high surface area) >  $\text{TiO}_2$  (rutile) >  $\text{TiO}_2$  (anatase, rutile) >  $\gamma\text{-Al}_2\text{O}_3$  >  $\text{SiO}_2$  >  $\text{TiO}_2$  (anatase, low surface area).<sup>103</sup> In addition, by modifying the  $\text{TiO}_2$  support with a

small amount of  $\text{CeO}_2$ , the performance could be further enhanced.<sup>61</sup>

Ce-Zr solid solutions are a special type of support due to their positive cooperation with active sites and have been widely used as catalyst supports for metal oxides. Gao et al. investigated the effect of the morphology  $\text{ZrO}_2\text{-CeO}_2$  on the performance of MnOx/ $\text{ZrO}_2\text{-CeO}_2$  catalysts for the selective catalytic reduction of NO with ammonia. As shown in Figure 2a, the catalytic tests showed that MnOx/ $\text{ZrO}_2\text{-CeO}_2$  nanorods achieved significantly higher NO conversion than the nanocubes or nanopolyhedra.<sup>85</sup> The apparent activation energy of the nanorods is 25 kJ/mol, which was much lower than the values of the nanocubes or nanopolyhedra (42 and 43 kJ/mol).  $\text{ZrO}_2\text{-CeO}_2$  nanorods had a strong interaction with MnOx species, which resulted in the superior selective catalytic reduction of NO. Furthermore, MnOx can be highly dispersed on the surface of  $\text{Ce}_{0.9}\text{Zr}_{0.1}\text{O}_2$  nanorods (shown in Figure 2b). Various species, such as  $\text{Mn}^{2+}$ ,  $\text{Mn}^{3+}$ , and  $\text{Mn}^{4+}$ , were observed due to the strong interaction between manganese and cerium oxide. The MnOx/ $\text{Ce}_{0.9}\text{Zr}_{0.1}\text{O}_2$  nanorods exhibited an NO conversion greater than 90% at 150  $^{\circ}\text{C}$ .

Carbon-based materials have high surface areas and excellent electron transfer performances, which are favorable for MnOx support. Recently, researchers have studied the novel CNT support for the modification of MnOx. Wang et al. synthesized a series of MnOx supported multiwalled carbon nanotubes (MWCNTs). Manganese species existed in the  $\text{MnO}_2$ ,  $\text{Mn}_3\text{O}_4$ , and MnO state in the MnOx/MWCNTs catalysts, and most of the Mn existed as  $\text{MnO}_2$  and  $\text{Mn}_3\text{O}_4$ . MWCNTs (60–100 nm) supporting 10 wt % manganese catalysts calcined at 400  $^{\circ}\text{C}$  catalyst presented the best SCR activity under the conditions of 1000 ppm of  $\text{NH}_3$ , 1000 ppm of NO and 5 vol %  $\text{O}_2$ . Well-dispersed MnOx on the MWCNTs, a high concentration of  $\text{MnO}_2$ , and a low concentration of MnO would lead to high SCR activity.<sup>97</sup>

MnOx-X is a series of composite manganese oxides that have high activity for NO. The X can be  $\text{CeO}_2$ ,<sup>58,60,95,104-108</sup> Fe-Mn mixed oxide catalysts,<sup>109-111</sup> Cu-Mn mixed oxides,<sup>112</sup> V-Mn mixed oxides,<sup>113</sup> W-Mn mixed oxides,<sup>114</sup> Ni-Mn mixed oxides,<sup>115-117</sup> Co-Mn mixed oxides,<sup>118</sup> Zr-Mn mixed oxides,<sup>119,120</sup> and Ca-modified MnOx.<sup>121</sup>

Ce is the most used element for the modification of MnOx.<sup>122</sup>  $\text{CeO}_2$  is well-known to have labile oxygen vacancies and bulk oxygen species with relatively high mobility. In addition, it is easily formed during the redox shift between  $\text{Ce}^{4+}$  and  $\text{Ce}^{3+}$  under oxidizing and reducing conditions, respectively. Cooperation with MnOx could enhance the performance of MnOx, and the mechanism has also been widely studied. To further enhance the performance of Ce-MnOx mixed oxides,

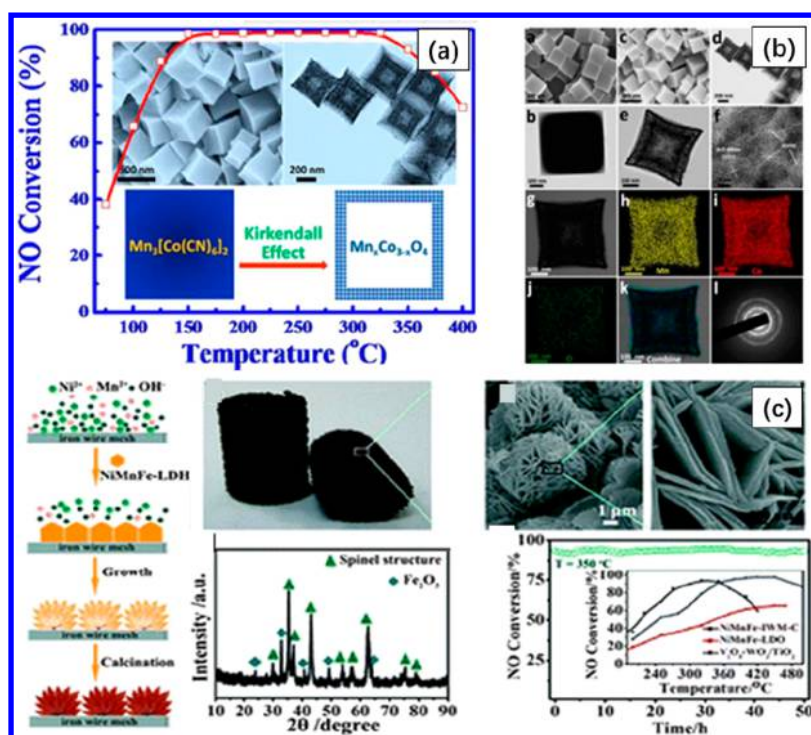


Figure 3. Performance of NO removal over (a) Co–Mn mixed oxide,<sup>118</sup> (b) and (c) Ni–Mn–Fe mixed oxide.<sup>124</sup>

the catalyst having a Sn/Mn/Ce = 1:4:5 molar ratio showed the greatest improvement in SCR activity, with near 100% NO<sub>x</sub> conversion at 110–230 °C.<sup>56,58</sup> In addition, Sn-modified MnO<sub>x</sub>-CeO<sub>2</sub> showed remarkably improved tolerance to SO<sub>2</sub> sulfonation and to the combined effect of SO<sub>2</sub> and H<sub>2</sub>O. In the presence of SO<sub>2</sub> and H<sub>2</sub>O, the Sn-modified MnO<sub>x</sub>-CeO<sub>2</sub> catalyst gave 62% and 94% NO<sub>x</sub> conversions compared to 18% and 56% over MnO<sub>x</sub>-CeO<sub>2</sub> at temperatures of 110 and 220 °C, respectively. In addition, a ternary oxide was further developed to enhance the performance, and the Mn–Ce–Ti catalyst exhibited excellent NH<sub>3</sub>-SCR activity and strong resistance against H<sub>2</sub>O and SO<sub>2</sub> over a broad operation temperature window. From characterization of the catalyst, it was found that the dual redox cycles (Mn<sup>4+</sup> + Ce<sup>3+</sup> ↔ Mn<sup>3+</sup> + Ce<sup>4+</sup> and Mn<sup>4+</sup> + Ti<sup>3+</sup> ↔ Mn<sup>3+</sup> + Ti<sup>4+</sup>) and the amorphous structure play key roles in the high catalytic performance in de-NO<sub>x</sub>.<sup>123</sup>

As shown in Figure 3a, mixed metal oxides with different morphologies were synthesized for use in the NH<sub>3</sub>-SCR reaction. Hollow, porous Mn<sub>x</sub>Co<sub>3-x</sub>O<sub>4</sub> nanocages were synthesized via a self-assembly method, with a spinel structure that was thermally derived from nanocube-like metal–organic frameworks (Mn<sub>3</sub>[Co(CN)<sub>6</sub>]<sub>2</sub>·nH<sub>2</sub>O). Such hollow and porous structures provide larger surface areas and more active sites to adsorb and activate reaction gases, resulting in high catalytic activity.<sup>118</sup> In addition, the catalysts have high cycle stability and good SO<sub>2</sub> tolerance due to the uniform distribution and strong interaction of the manganese and cobalt oxide species. Figure 3b exhibits a novel class of monolithic Ni–Mn–Fe mixed metal oxides. The materials were grown in situ on iron wire meshes in a cylindrical form and show high catalytic activity and ~100% selectivity for N<sub>2</sub> in the SCR of NO with NH<sub>3</sub>. These catalysts presented uniform 3D flower-like nanoarrays with a homogeneous distribution of active components and good binding of the active material with the iron substrate, ideally allowing their

catalytic properties to be maintained under harsh reaction conditions.<sup>125</sup>

Some special crystalline MnO<sub>x</sub> materials have unique performances in the NH<sub>3</sub>-SCR reaction. As of now, only perovskite oxides, Fe–Mn spinel oxides,<sup>126,127</sup> and MnZr<sub>2</sub>O<sub>4</sub> spinel oxides<sup>128</sup> have been synthesized for this reaction. Perovskite oxides are the most widely used materials for NH<sub>3</sub>-SCR due to their high catalytic oxidation performance. LaMnO<sub>3</sub> can achieve catalysis with NO conversions higher than 70% at 200–300 °C, showing the great contribution of the perovskite crystal structure to the SCR performance.<sup>12</sup> Li et al. prepared a series of attapulgite-supported perovskite-type La<sub>1-x</sub>Ce<sub>x</sub>MnO<sub>3</sub> ( $x = 0-0.2$ ) using a sol-gel method.<sup>129</sup> La<sub>1-x</sub>Ce<sub>x</sub>MnO<sub>3</sub> nanoparticles approximately 15 nm in size and were uniformly immobilized on the surface of attapulgite with a loading amount of 20 wt %. When the doping fraction  $x$  was 0.1, the catalyst showed the highest NO conversion rate of 98.6%. The attapulgite support supplied a high surface area, facilitating nanoparticle dispersion as well as gas adsorption.

Various types of manganese oxides have been developed for selective catalytic reduction of NO<sub>x</sub> with NH<sub>3</sub>. Future work should focus on improving nitrogen selection and enhancing SO<sub>2</sub> resistance at a low temperature based on promising MnO<sub>x</sub>.

**3.2. Catalytic Combustion of VOCs.** VOCs are hazardous air pollutants because of their toxic, malodorous, mutagenic, and carcinogenic properties. They are also ozone and smog precursors.<sup>130,131</sup> Catalytic combustion is an efficient method for VOC control. At present, supported noble metals (Pt and Pd) and metal oxide catalysts are used for the reduction of VOC emissions.<sup>132</sup> In particular, transition metal oxides have shown very good catalytic performances in oxidation reactions.

Manganese oxides, such as Mn<sub>3</sub>O<sub>4</sub>, Mn<sub>2</sub>O<sub>3</sub>, and MnO<sub>2</sub>, are known to exhibit high activity in the oxidation of hydrocarbons. Sang et al. investigated the catalytic combustion performance of VOCs (benzene and toluene) over pure manganese oxide catalysts (Mn<sub>3</sub>O<sub>4</sub>, Mn<sub>2</sub>O<sub>3</sub>, and MnO<sub>2</sub>). The results indicated

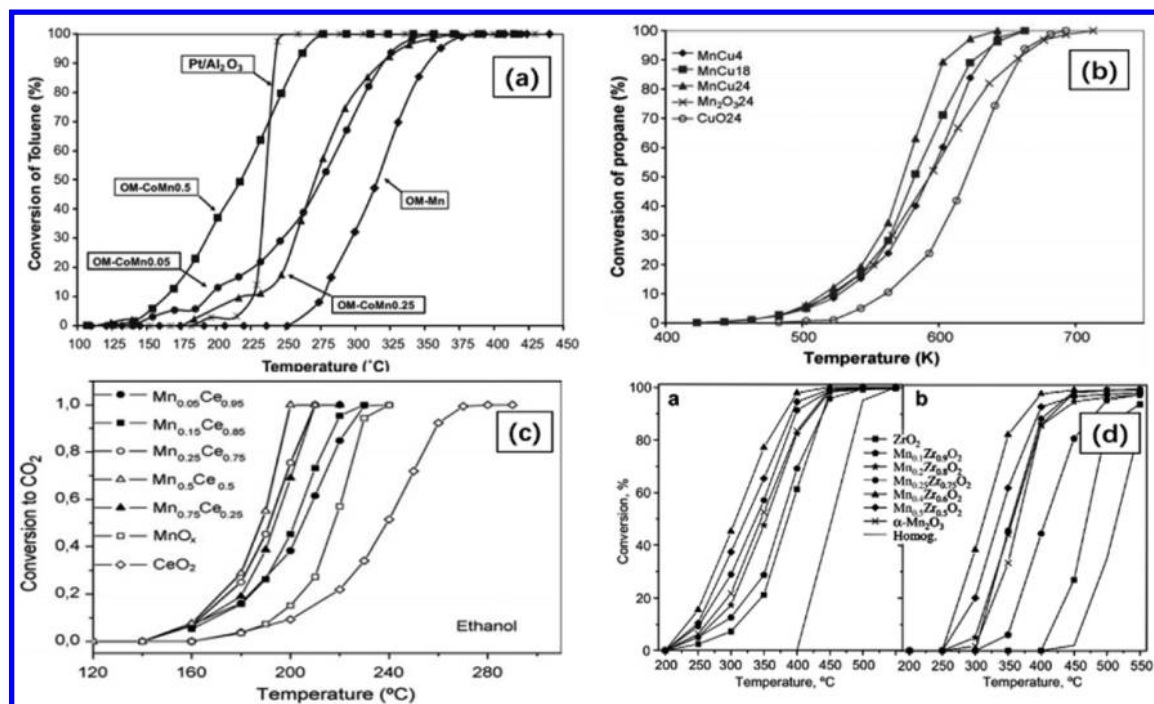


**Figure 4.** (a) Conversion of toluene over Co-MnOx mixed oxides.<sup>135</sup> (b) Catalytic activity in the total oxidation of propane over Cu-Mn mixed oxides.<sup>136</sup> (c) Conversion of ethyl acetate to CO<sub>2</sub> over Mn-Ce catalysts.<sup>137</sup> (d) Light-off curves of the combustion of DCE and TCE over Mn<sub>x</sub>Zr<sub>1-x</sub>O<sub>2</sub> catalysts.<sup>55</sup>

that the sequence of catalytic activity was Mn<sub>3</sub>O<sub>4</sub> > Mn<sub>2</sub>O<sub>3</sub> > MnO<sub>2</sub>, which was correlated with oxygen mobility on the catalyst. Furthermore, the effects of alkaline metals and alkaline earth metals on MnOx were also studied. K, Ca, and Mg seemed to act as promoters, and the promoting effect might be ascribed to oxide defect- or hydroxyl-like groups.<sup>133</sup>

There are only a few studies that report supported MnOx materials for the catalytic combustion of VOCs. Al<sub>2</sub>O<sub>3</sub>-supported MnOx was prepared and tested for the combustion of formaldehyde. The results indicated that the total combustion of formaldehyde/methanol was achieved at 220 °C over a 18.2% Mn/Al<sub>2</sub>O<sub>3</sub> catalyst.<sup>134</sup> Mn was indicated to be the primary active site for the reaction.

Mixed metal oxides have been widely applied in the catalytic combustion of VOCs.<sup>138</sup> Transition metal oxides, rare earth elements, and main groups elements were selected for the modification of MnOx. Cu-MnOx and Co-MnOx mixed binary oxides were synthesized from hydrotalcites to remove VOCs (toluene, ethanol, and butanol). The results indicated that all of these binary metal oxides have activity in the oxidation reaction of VOCs. However, the difficulty to oxidize these organic compounds was in the order of butanol < ethanol < toluene. As shown in Figure 4a, among these binary metal oxides, the Co-MnOx catalyst had the highest activity, which was due to the generation of amorphous phases and redox cycles as a consequence of the cooperative effect among the metals.<sup>135</sup> Cu-MnOx mixed oxides were also synthesized for the catalytic combustion of propane and ethanol. The mixed oxides were prepared through coprecipitation by varying the aging time for 4, 18, and 24 h. Figure 4b gives the results of the catalytic activity of Cu-Mn mixed oxides in the total oxidation of propane. The results indicated that the catalytic performance of Cu-MnOx binary metal oxides was better than that of pure Mn<sub>2</sub>O<sub>3</sub> and CuO oxides. Furthermore, an increase in aging time could enhance activity and selectivity for CO<sub>2</sub>.<sup>136</sup> The Ce-

MnOx mixed oxide was the most useful catalyst for VOC removal. MnOx-CeO<sub>2</sub> catalysts were prepared for the oxidation of ethanol. Mn was present in the Mn<sup>2+</sup> and Mn<sup>3+</sup> state on the surface. Crystalline manganese oxide phases are absent in ceria-rich materials, while the Mn<sub>3</sub>O<sub>4</sub> phase is present in manganese-rich materials. Mn ions were highly dispersed in the ceria structure, resulting in the larger surface area of the MnOx-CeO<sub>2</sub> catalysts than compared to that of the single oxide prepared using the same method. The larger surface area of the MnOx-CeO<sub>2</sub> catalysts contributes to the higher activity. As shown in Figure 4c, among all the catalysts, the Mn<sub>0.5</sub>Ce<sub>0.5</sub> sample is the most active, and at temperatures lower than 200 °C, all of the ethyl acetate can be converted to CO<sub>2</sub>.<sup>139</sup> Mn-Zr mixed oxides were used in the catalytic combustion of chlorocarbons. 1,2-Dichloroethane (DCE) and trichloroethylene (TCE) were selected as target pollutants. As shown in Figure 4d, the mixed oxide with 40 mol % manganese was found to be an optimum catalyst for the combustion of both chlorocarbons with a T<sub>50</sub> value of approximately 305 and 315 °C for DCE and TCE oxidation, respectively. The excellent activity of the Mn-Zr mixed oxides was ascribed to their substantial surface acidity combined with readily accessible active oxygen species. Furthermore, it was observed that the product formation of both CO<sub>2</sub> and Cl<sub>2</sub> was promoted with Mn loading.<sup>140</sup>

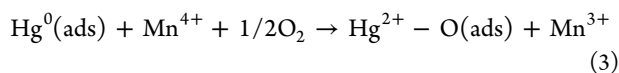
In addition, some ternary Mn-based composite oxides are often selected for VOC combustion. Ce-Zr mixed oxides were also synthesized using a sol-gel method. The prepared Zr<sub>0.4</sub>Ce<sub>0.6-x</sub>Mn<sub>x</sub>O<sub>2</sub> catalyst has a very high surface specific area, small crystallite size, and good redox properties. With increasing Mn content in the composite, the textural and redox properties were improved, especially for x = 0.36. The experimental results showed that the most active and selective catalyst in butanol oxidation was obtained for the nominal composition Zr<sub>0.4</sub>Ce<sub>0.24</sub>Mn<sub>0.36</sub>O<sub>2</sub> due to its high oxygen mobility and surface Mn<sup>4+</sup> concentration.<sup>141</sup> Cu modified

Mn–Ce mixed oxides were also synthesized for various types of VOCs.  $\text{Cu}_{0.15}\text{Mn}_{0.3}\text{Ce}_{0.55}$ /cordierite showed higher activities than commercial Pd/ $\text{Al}_2\text{O}_3$  for the combustion of various types of VOCs, especially for oxygen-derived compounds that could be lighted off below 200 °C.<sup>142</sup>

Perovskite oxides have been used for the catalytic combustion of VOCs.<sup>54,143</sup> Nanosized perovskite-type oxides of  $\text{La}_{1-x}\text{Sr}_x\text{MO}_{3-\delta}$  ( $M = \text{Co}, \text{Mn}; x = 0, 0.4$ ) were prepared using the citric acid complexing-hydrothermal-coupled method. The high surface areas, good redox properties (derived from higher  $\text{Mn}^{4+}/\text{Mn}^{3+}$  and  $\text{Co}^{3+}/\text{Co}^{2+}$  ratios), and rich lattice defects of the nanostructured  $\text{La}_{1-x}\text{Sr}_x\text{MO}_{2-\delta}$  materials contributed to the excellent catalytic performance.<sup>93</sup>

**3.3.  $\text{Hg}^0$  Oxidation and Adsorption.** Elemental mercury ( $\text{Hg}^0$ ), mainly existing in the atmosphere, is a major pollutant in the environment.<sup>144–146</sup> Coal-fired power plants are regarded as the largest stationary source for  $\text{Hg}^0$  emission.<sup>147</sup> Mercury exists in the flue gas mainly as  $\text{Hg}^0$ , oxidized mercury ( $\text{Hg}^{2+}$ ), and particle-bound mercury ( $\text{Hg}^p$ ). In general,  $\text{Hg}^{2+}$  and  $\text{Hg}^p$  can be removed by current technologies, such as wet desulphurization device (WFGD) and fiber filter/electrostatic precipitators (FF/ESP) devices.<sup>148</sup> However,  $\text{Hg}^0$  is hard to remove due to the high volatility and low insolubility in water.<sup>147</sup>

Lots of work has been done to develop novel catalysts or sorbents for the conversion of  $\text{Hg}^0$  to  $\text{Hg}^{2+}/\text{Hg}^p$ . Among various materials, Mn-based oxide is one of the efficient  $\text{Hg}^0$  removal catalysts or sorbents due to its high redox potential, environmental friendliness, and low cost. For a  $\text{Hg}^0$  removal mechanism over MnOx, a simple description is as follows: the gaseous  $\text{Hg}^0$  is first adsorbed on the surface of MnOx, and after that, the  $\text{Hg}^0$  is oxidized to  $\text{Hg}^{2+}$  by the oxidation performance of high valence of ( $\text{Mn}^{4+}/\text{Mn}^{3+}$ ). After catalytic oxidation, most of the oxidized mercury is captured by MnOx.<sup>147</sup> The oxidized mercury combines with the surface oxygen of MnOx. During this reaction, the large surface area is favorable for  $\text{Hg}^0$  adsorption, high catalytic oxidation performance is useful for  $\text{Hg}^0$  oxidation, and the sufficient surface oxygen benefits  $\text{Hg}^{2+}$  binding. The basic mechanism can be illustrated as follows:



Xu et al. synthesized one-dimensional  $\alpha$ -,  $\beta$ -, and  $\gamma$ - $\text{MnO}_2$  for  $\text{Hg}^0$  removal.<sup>29</sup> As shown in Figure 5, the results indicated that the performance of  $\text{Hg}^0$  removal was enhanced in the order of  $\beta$ - $\text{MnO}_2 < \gamma$ - $\text{MnO}_2 < \alpha$ - $\text{MnO}_2$ . The crystal structure has a significant effect on  $\text{Hg}^0$  catalytic oxidation. The mechanism for  $\text{Hg}^0$  capture was ascribed to the  $\text{Hg}^0$  catalytic oxidation with the reduction of  $\text{Mn}^{4+} \rightarrow \text{Mn}^{3+} \rightarrow \text{Mn}^{2+}$ . After  $\text{Hg}^0$  oxidation, the oxidized mercury combined with surface oxygen of  $\text{MnO}_2$ . Furthermore, the interaction forces between mercury and manganese oxide sites are demonstrated to increase in the following order:  $\beta$ - $\text{MnO}_2 < \gamma$ - $\text{MnO}_2 < \alpha$ - $\text{MnO}_2$  based on the desorption tests.

Supported Mn-based oxides have been widely studied for  $\text{Hg}^0$  removal.  $\text{Al}_2\text{O}_3$ ,<sup>149–151</sup>  $\text{TiO}_2$ ,<sup>7,149,152–154</sup> AC,<sup>155</sup> fly ash,<sup>156</sup> graphene,<sup>30</sup> CNTs,<sup>157</sup> Ce–Zr solid solutions,<sup>158</sup>  $\gamma$ - $\text{Fe}_2\text{O}_3$ <sup>159</sup> and SCR catalysts are often used as catalyst supports. On the basis of their properties, the support can be classified into two categories: (1) Supports in the first category have no reaction activity with  $\text{Hg}^0$ , such as  $\text{Al}_2\text{O}_3$ ,  $\text{TiO}_2$ , CNTs, graphene, and

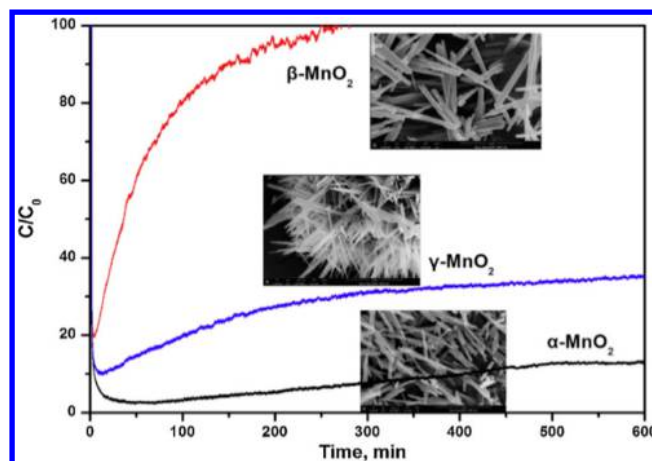


Figure 5. Performance of  $\text{Hg}^0$  removal over different one-dimensional  $\alpha$ -,  $\beta$ -, and  $\gamma$ - $\text{MnO}_2$ .<sup>29</sup>

Ce–Zr solid solutions. Although these materials have no activity for  $\text{Hg}^0$  removal, the supports are beneficial for the dispersion of MnOx particles.  $\text{TiO}_2$  is a useful support for MnOx. The BET surface area can be enlarged by  $\text{TiO}_2$ . Recent studies have examined Ce–Zr solid solutions. Ce–Zr solid solutions can enhance the amount of the surface oxygen on MnOx, which is favorable for the catalytic oxidation of  $\text{Hg}^0$ . Novel CNT and graphene materials have also been selected as supports for MnOx and used for  $\text{Hg}^0$  adsorption. CNTs and graphene have no  $\text{Hg}^0$  removal efficiency. However, after synthesis with these materials, the manganese oxide particles decreased in size and were uniformly dispersed, which enhanced the  $\text{Hg}^0$  removal performance. The second category includes catalytic supports, such as AC, SCR catalysts,  $\gamma$ - $\text{Fe}_2\text{O}_3$ , and fly ash. AC and fly ash show performance in  $\text{Hg}^0$  adsorption, where after Mn-modification, mercury existed in a chemically adsorbed state, which highly enhanced the  $\text{Hg}^0$  adsorption performance. SCR catalysts ( $\text{V}-\text{W}-\text{Ti}/\text{V}-\text{Mo}-\text{Ti}$ ) for the  $\text{NH}_3$ -SCR reaction also have  $\text{Hg}^0$  catalytic oxidation performance to some extent. With the addition of MnOx, their performance in  $\text{Hg}^0$  removal can be enhanced, especially at low temperature.  $\gamma$ - $\text{Fe}_2\text{O}_3$  and some other transition metal oxides are often used as  $\text{Hg}^0$  sorbents. Their mercury capacities are usually lower than that of MnOx. However, the interaction between MnOx and the support benefits the  $\text{Hg}^0$  reaction. Furthermore, the magnetic materials offer the possibility to recycle the spent sorbent from the fly ashes.

MnOx-X composites have been used for the modification of MnOx. MnOx-X can be Ce-MnOx,<sup>8,154,160</sup> Mo-MnOx,<sup>157</sup> Fe-MnOx,<sup>161,162</sup> Zr-MnOx,<sup>163</sup> or Sn-MnOx.<sup>164,165</sup> Ce is the most used element for the modification of MnOx. The oxygen storage performance of  $\text{CeO}_2$  is beneficial for catalytic oxidation and mercury adsorption. Iron metal oxides show performance in  $\text{Hg}^0$  removal, and the Fe–Mn binary material can synergetically enhance the  $\text{Hg}^0$  removal performance. The main group element Zr has also been used for the modification of MnOx to enhance the capacity. Sn can enlarge the reaction temperature window. Complex metal oxides, such as Fe–Sn-modified, can enhanced the  $\text{Hg}^0$  capacity as well as  $\text{SO}_2$  resistance.

Sometimes, the materials contain elements that modify MnOx and the catalyst support. As shown in Figure 6, Mn–Ce/Ti-PILC (PILCs, pillared interlayered clays) catalysts were prepared for the simultaneous removal of NO and  $\text{Hg}^0$  in

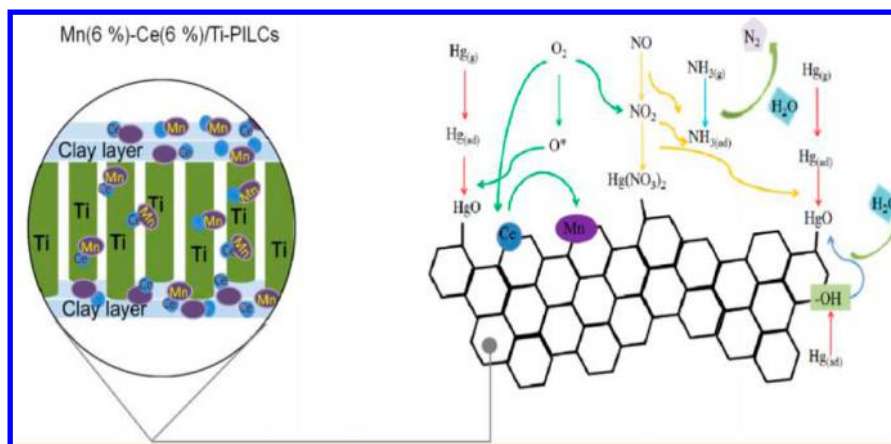
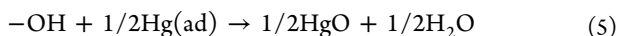


Figure 6.  $\text{Hg}^0$  removal mechanism over Mn–Ce/Ti-PILCs.<sup>166</sup>

simulated flue gas.<sup>166</sup> The results indicated that the Mn–Ce/Ti-PILCs were highly promising for controlling the emission of NO and mercury. The mechanism for the simultaneous removal of NO and  $\text{Hg}^0$  over Mn–Ce/Ti-PILC catalysts was as follows:



Some special crystal  $\text{MnO}_x$ , Fe–Mn spinel,<sup>167,168</sup> and perovskite oxide<sup>14</sup> were also used as catalysts for  $\text{Hg}^0$  removal in recently studies. Yang et al. used a novel magnetic Fe–Ti–V spinel catalyst for  $\text{Hg}^0$  removal, the results indicated that such material has an excellent performance for elemental mercury capture at 100 °C, and the formed  $\text{HgO}$  can be catalytically decomposed by the catalyst at 300 °C to reclaim elemental mercury and regenerate the catalyst.<sup>67</sup> Xu et al. use  $\text{LaMnO}_3$  perovskite oxide for the simultaneous removal  $\text{Hg}^0$  and  $\text{NO}_x$  at low temperature.  $\text{LaMnO}_3$  not only has the low temperature  $\text{NH}_3$ –SCR for  $\text{NO}_x$  removal performance, but also has a high  $\text{Hg}^0$  adsorption capacity. The  $\text{Hg}^0$  capacity of  $\text{LaMnO}_3$  is as high as 6.22 mg/g (600 min) at 150 °C.<sup>169</sup> In the future work, a Mn-based sorbent which has large mercury capacity as well as  $\text{SO}_2$  and  $\text{H}_2\text{O}$  resistance should be further developed.

**3.4. Soot Oxidation.** Nano-/microparticles of carbon (soot) emitted by diesel engines is a current environmental problem.<sup>170</sup> Vehicle manufactures have done much work to eliminate the hazard of soot emission. Generally, soot can be removed from gas streams with so-called diesel particulate filters (DPFs). In this process, the catalytic combustion of such carbon particles has been proposed for the regeneration of the DPF in order to avoid a pressure drop in the exhaust. Diesel engine exhausts have a high concentration of  $\text{O}_2$  (5–20%), along with a certain proportion of  $\text{NO}_x$  (0.01–0.1%), which is mainly emitted as NO. Therefore, a catalyst for soot removal should be active in such oxidizing atmospheres. Several manganese oxides, such as mixed oxides or perovskite-like oxides, have been shown to be effective for the catalytic combustion of soot.

Figure 7 gives the soot oxidation performances for several Mn-based oxides. Clearly, these Mn-based oxides showed quite different performances, and the catalytic activity followed the trend: birnessite > cryptomelane >  $\text{Mn}_3\text{O}_4$  >  $\text{Mn}_2\text{O}_3$  > natural  $\text{MnO}_2$  >  $\text{MnO}_2 = \text{MnO}$ .<sup>172</sup> Legutko et al. investigated K-doped manganese spinel, and the results indicated that K-doped  $\text{Mn}_3\text{O}_4$  at low loadings (0.5 ML) has a negative effect on

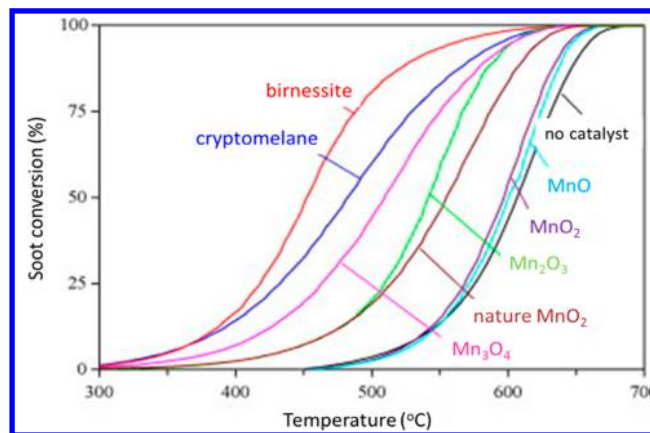


Figure 7. Soot oxidation performance over Mn-based oxides.<sup>171</sup>

catalysis, whereas at high loadings (9 ML), it leads to the formation of a birnessite shell on the  $\text{Mn}_3\text{O}_4$  core catalyst accompanied by a spectacular increase in the soot oxidation rate ( $\Delta T_{50\%} \approx 150$  °C).<sup>173</sup> Steffen et al. investigated the catalytic oxidation of soot by  $\text{O}_2$  on bare manganese oxides.  $\text{MnO}_2$ ,  $\text{Mn}_2\text{O}_3$ , and  $\text{Mn}_3\text{O}_4$ , as well as nanosized  $\text{Mn}_3\text{O}_4$ , originating from flame spray pyrolysis (FSP- $\text{Mn}_3\text{O}_4$ ), were tested. FSP- $\text{Mn}_3\text{O}_4$  showed the best performance among the tested samples. The catalyst revealed high efficiency for close contact, yielding peak  $\text{CO}_2$  at 305 °C.<sup>174</sup>

Hydrotalcite-based  $\text{Mn}_x\text{Mg}_{3-x}\text{AlO}$  catalysts were synthesized for soot combustion,  $\text{NO}_x$  storage, and simultaneous soot- $\text{NO}_x$  removal. It was indicated that with an increase in Mn content in the hydrotalcite-based  $\text{Mn}_x\text{Mg}_{3-x}\text{AlO}$  catalysts, the major Mn-related species varied from  $\text{MnAl}_2\text{O}_4$  and  $\text{Mg}_2\text{MnO}_4$  to  $\text{Mn}_3\text{O}_4$  and  $\text{Mn}_2\text{O}_3$ .<sup>175</sup> The catalyst  $\text{Mn}_{1.5}\text{Mg}_{1.5}\text{AlO}$  displays the highest soot combustion activity, and the temperature for the maximal soot combustion rate decreased by 210 °C.

Ce-based or Ce–Zr mixed oxide supports for Mn oxide were also used for soot oxidation.<sup>176</sup>  $\text{MnO}_x$ – $\text{CeO}_2$  mixed oxides were introduced into a Pt/ $\text{Al}_2\text{O}_3$  catalyst. The modified catalyst exhibited a high thermal stability with a  $T_{50}$  increase from 442 to 460 °C after calcination in air at 800 °C for 100 h, which is attributed to the stabilization effect of alumina on  $\text{MnO}_x$ – $\text{CeO}_2$ . After modification, the amount of platinum was reduced, and the catalytic activity was improved for soot oxidation in the presence of  $\text{NO}_x$ .<sup>177</sup>

Liang et al. prepared Mn–Ce mixed oxides and investigated the role of Mn and Ce. As shown in Figure 8a, the results

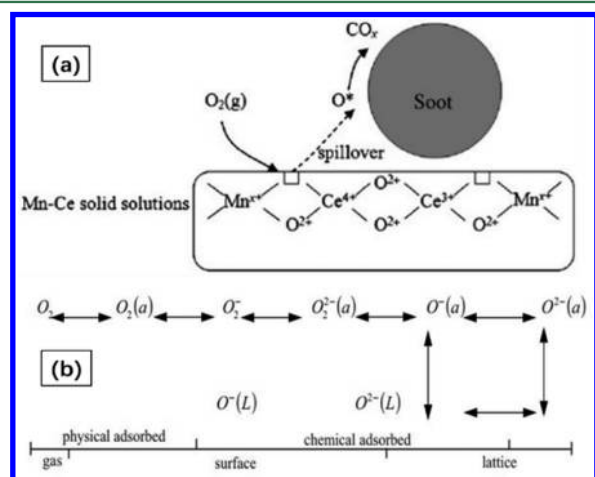


**Figure 8.** (a) Reaction mechanism and active oxygen species of the Mn–Ce mixed oxides under loose contact conditions.<sup>178</sup> (b) The different adsorption states of oxygen gas on the surface of the catalysts.<sup>179</sup>

indicated that Mn<sup>x+</sup> cations entered into the ceria lattice to form solid solutions. Such structures can increase the amount of oxygen vacancies and promote surface oxygen chemisorption.<sup>178</sup> In addition, by trapping electrons, oxygen adsorption leads to the formation of O<sup>2-</sup>, which is the active center for oxidation. The surface oxygens exist as physically adsorbed and chemically adsorbed oxygen. In Mn-based oxides, the surface oxygen adsorption states appear in three stages, as shown in Figure 8b, where O<sub>2</sub>(a) changed from O<sub>2</sub> to O<sub>2</sub><sup>-</sup> and then to O<sup>2-</sup>, along with the activity from weak to strong.

To further enhance the performance of Ce–Mn mixed oxides, the introduction of Al<sub>2</sub>O<sub>3</sub> may degrade the soot oxidation activity compared with MnOx–CeO<sub>2</sub> mixed oxides. However, the surface area of the catalyst was enlarged, and a high MnOx dispersion was produced after rigorous aging treatment. As a result, the prepared MnCe/Al catalyst exhibits the highest thermal stability, with a small increase in *T*<sub>m</sub> of 17 °C.<sup>62</sup> Wu et al. investigated the effect of gases on soot oxidation over Mn–Ce mixed oxides. It was found that among the catalysts investigated, the MnOx–CeO<sub>2</sub> mixed oxide catalyst presents the lowest soot oxidation temperature in the presence of NO and O<sub>2</sub>.<sup>180</sup> A Ba/MnCe ternary catalyst was prepared by impregnating barium acetate on MnOx–CeO<sub>2</sub> mixed oxides. The soot oxidation activities were evaluated in the presence of NO under an energy transfer controlled regime. Ba/MnCe presented the lowest maximal soot oxidation rate temperature of 393 °C among the prepared catalysts.<sup>181</sup> In addition, about half of the nitrates stored on this catalyst decomposed within the temperature interval of 350–450 °C. The ignition temperature of soot decreased significantly with the involvement of nitrates or NO<sub>2</sub> release.

An Mn-based perovskite oxide was also prepared for soot oxidation. LaMnO<sub>3</sub> perovskite oxide can capture effect soot and has catalytic activity in soot combustion. The porous structural characteristics of LaMnO<sub>3</sub> contribute to the soot capture as well as the catalytic performance in soot combustion, which is largely affected by the chemical composition, grain size, specific surface area, and pore structure, which are related to ion substitution and calcination temperature.<sup>182</sup> Mixed perovskite

oxides in the La–K–Mn–O system were synthesized and investigated for catalytic activity toward simultaneous soot–NOx removal.<sup>183</sup> The mixed oxides showed good activity for NOx and soot removal, and the activity and NOx reduction selectivity depended significantly on the K content.

**3.5. Application to Other Reactions.** Besides the above-mentioned reactions, the Mn-based oxides are also promising catalysts for some other reactions, such as CO oxidation<sup>184,185</sup> and H<sub>2</sub>S sorption.<sup>186</sup> Catalytic oxidation of CO has been established for exhaust gas cleaning.<sup>185</sup> Gold-supported MnOx,<sup>184</sup> Ag-modified MnOx,<sup>187</sup> Cu–MnOx mixed oxides,<sup>185</sup> MnOx-modified Co<sub>3</sub>O<sub>4</sub>–CeO<sub>2</sub> catalysts,<sup>188</sup> etc. were investigated for CO oxidation. Hydrogen sulfide (H<sub>2</sub>S) emitted from the hot fuel gas which was produced during gasification of coal and other fossil fuels. The H<sub>2</sub>S sorption rate observed at 600 °C with the Ce–Mn mixed oxide material was also found to be higher than that of Zn–Mn, V–Mn, and Fe–Mn mixed oxide materials.<sup>189</sup> We refer the reader to the literature, and we believe that the applications were not merely like we described.

## 4. SUMMARY AND PERSPECTIVE

We give a brief survey of different types of manganese oxides in the application of selective catalytic reduction of NOx with NH<sub>3</sub>, the catalytic combustion of VOCs, Hg<sup>0</sup> oxidation and adsorption, and soot oxidation. In these heterogeneous catalytic reactions, manganese oxides exhibited various functions. Pure MnOx is favorable for a better understanding of catalytic reaction mechanism. MnOx/support can enlarge the surface area and improve some physical or chemical properties. MnOx–X composites are promising materials for the application in various conditions. MnOx–S are potential materials that make full use of their own characteristics. The combination of these types of manganese will meet the strict demands.

However, many manganese oxides have limitations when used, such as (1) particle aggregation; (2) easily poisoned by SO<sub>2</sub> and H<sub>2</sub>O; and (3) low electron conductivity. To solve the first problem, supported manganese oxides were selected for high dispersion of Mn active sites. Some complex manganese oxides such as Ce–MnOx, Sn–MnOx, and Fe–MnOx were synthesized to enhance their performances when used. Some carbon materials were added to Mn-based oxides to enhance the electron conductivity. Although much work had been done to solve these problems, there is still no suitable method that can give an exciting result. Furthermore, ongoing and future efforts should pay more attention to how to prepare a more efficient manganese oxide in order to commercialize it for industrial use.

## ■ AUTHOR INFORMATION

### Corresponding Author

\*Tel: +86-021-54745591. Fax: +86-54745591. E-mail: [nqyan@sjtu.edu.cn](mailto:nqyan@sjtu.edu.cn).

### ORCID

Naiqiang Yan: 0000-0003-3736-4548

### Notes

The authors declare no competing financial interest.

## ■ ACKNOWLEDGMENTS

This study was supported by the Major State Basic Research Development Program of China (973 Program, No. 2013CB430005), the National Natural Science Foundation of China (No. 51478261 and No.51278294). This study was also

supported by Postdoctoral Innovative Talents Plan (No. BX201700151).

## ■ REFERENCES

- (1) Shen, Y. F.; O'Young, C. L.; Zerger, R. P.; DeGuzman, R. N.; Suib, S. L.; McCurdy, L.; Potter, D. I. Manganese Oxide Octahedral Molecular Sieves: Preparation, Characterization, and Applications. *Science* **1993**, *260* (5107), 511–515.
- (2) Post, J. E. Manganese oxide minerals: Crystal structures and economic and environmental significance. *Proc. Natl. Acad. Sci. U. S. A.* **1999**, *96* (7), 3447–3454.
- (3) Wei, W.; Cui, X.; Chen, W.; Ivey, D. G. Manganese oxide-based materials as electrochemical supercapacitor electrodes. *Chem. Soc. Rev.* **2011**, *40* (3), 1697–1721.
- (4) Thackeray, M. M.; Johnson, C. S.; Vaughey, J. T.; Li, N. Hackney, S. A., Advances in manganese-oxide 'composite' electrodes for lithium-ion batteries. *J. Mater. Chem.* **2005**, *15* (23), 179–183.
- (5) Zhang, H.; Cao, G.; Wang, Z.; Yang, Y.; Shi, Z.; Gu, Z. Growth of Manganese Oxide Nanoflowers on Vertically-Aligned Carbon Nanotube Arrays for High-Rate Electrochemical Capacitive Energy Storage. *Nano Lett.* **2008**, *8* (9), 2664–8.
- (6) Lee, S. W.; Kim, J.; Chen, S.; Hammond, P. T.; Shao-Horn, Y. Carbon nanotube/manganese oxide ultrathin film electrodes for electrochemical capacitors. *ACS Nano* **2010**, *4* (7), 3889–96.
- (7) Ji, L.; Sreekanth, P. M.; Smirniotis, P. G.; Thiel, S. W.; Pinto, N. G. Manganese oxide/titania materials for removal of NO<sub>x</sub> and elemental mercury from flue gas. *Energy Fuels* **2008**, *22* (4), 2299–2306.
- (8) Qu, Z.; Xie, J.; Xu, H.; Chen, W.; Yan, N. Regenerable sorbent with a high capacity for elemental mercury removal and recycling from the simulated flue Gas at a low temperature. *Energy Fuels* **2015**, *29* (10), 6187–6196.
- (9) Li, J.; Chang, H.; Ma, L.; Hao, J.; Yang, R. T. Low-temperature selective catalytic reduction of NO<sub>x</sub> with NH<sub>3</sub> over metal oxide and zeolite catalysts—a review. *Catal. Today* **2011**, *175* (1), 147–156.
- (10) Jiao, F.; Frei, H. ChemInform Abstract: Nanostructured Cobalt and Manganese Oxide Clusters as Efficient Water Oxidation Catalysts. *Energy Environ. Sci.* **2010**, *3* (37), 1018–1027.
- (11) Tian, Z.-R.; Tong, W.; Wang, J.-Y.; Duan, N.-G.; Krishnan, V. V.; Suib, S. L. Manganese oxide mesoporous structures: mixed-valent semiconducting catalysts. *Science* **1997**, *276* (5314), 926–930.
- (12) Zhang, R.; Yang, W.; Luo, N.; Li, P.; Lei, Z.; Chen, B. Low-temperature NH<sub>3</sub>-SCR of NO by lanthanum Manganite perovskites: Effect of A-/B-site substitution and TiO<sub>2</sub>/CeO<sub>2</sub> support. *Appl. Catal., B* **2014**, *146* (3), 94–104.
- (13) Kim, S. C.; Shim, W. G. Catalytic combustion of VOCs over a series of manganese oxide catalysts. *Appl. Catal., B* **2010**, *98* (3–4), 180–185.
- (14) Xu, H.; Qu, Z.; Zong, C.; Quan, F.; Mei, J.; Yan, N. Catalytic oxidation and adsorption of Hg<sub>0</sub> over low-temperature NH<sub>3</sub>-SCR LaMnO<sub>3</sub> perovskite oxide from flue gas. *Appl. Catal., B* **2016**, *186*, 30–40.
- (15) Chen, S. Y.; Song, W.; Lin, H. J.; Wang, S.; Biswas, S.; Mollahosseini, M.; Kuo, C. H.; Gao, P. X.; Suib, S. L. Manganese Oxide Nanoarray-Based Monolithic Catalysts: Tunable Morphology and High Efficiency for CO Oxidation. *ACS Appl. Mater. Interfaces* **2016**, *8* (12), 7834–7842.
- (16) Ramesh, K.; Chen, L.; Chen, F.; Liu, Y.; Wang, Z.; Han, Y.-F. Re-investigating the CO oxidation mechanism over unsupported MnO, Mn<sub>2</sub>O<sub>3</sub> and MnO<sub>2</sub> catalysts. *Catal. Today* **2008**, *131* (1), 477–482.
- (17) Han, Y.-F.; Chen, F.; Zhong, Z.; Ramesh, K.; Chen, L.; Widjaja, E. Controlled synthesis, characterization, and catalytic properties of Mn<sub>2</sub>O<sub>3</sub> and Mn<sub>3</sub>O<sub>4</sub> nanoparticles supported on mesoporous silica SBA-15. *J. Phys. Chem. B* **2006**, *110* (48), 24450–24456.
- (18) Huo, Y.; Zhang, Y.; Xu, Z.; Zhu, J.; Li, H. Preparation of Mn<sub>2</sub>O<sub>3</sub> catalyst with core-shell structure via spray pyrolysis assisted with glucose. *Res. Chem. Intermed.* **2009**, *35* (6–7), 791–798.
- (19) Liang, S.; Teng, F.; Bulgan, G.; Zong, R.; Zhu, Y. Effect of phase structure of MnO<sub>2</sub> nanorod catalyst on the activity for CO oxidation. *J. Phys. Chem. C* **2008**, *112* (14), 5307–5315.
- (20) Débart, A.; Paterson, A. J.; Bao, J.; Bruce, P. G.  $\alpha$ -MnO<sub>2</sub> Nanowires: A Catalyst for the O<sub>2</sub> Electrode in Rechargeable Lithium Batteries. *Angew. Chem., Int. Ed.* **2008**, *47* (24), 4521–4.
- (21) Bai, B.; Li, J.; Hao, J.; Bai, B.; Hao, J. 1D-MnO<sub>2</sub>, 2D-MnO<sub>2</sub> and 3D-MnO<sub>2</sub> for low-temperature oxidation of ethanol. *Appl. Catal., B* **2015**, *164*, 241–250.
- (22) Yu, P.; Zhang, X.; Wang, D.; Wang, L.; Ma, Y. Shape-Controlled Synthesis of 3D Hierarchical MnO<sub>2</sub> Nanostructures for Electrochemical Supercapacitors. *Cryst. Growth Des.* **2009**, *9* (1), 528–533.
- (23) Wang, H.; Lu, Z.; Qian, D.; Li, Y.; Zhang, W. Single-crystal  $\alpha$ -MnO<sub>2</sub> nanorods: synthesis and electrochemical properties. *Nanotechnology* **2007**, *18* (11), 115616.
- (24) Wang, X.; Li, Y. Selected-Control Hydrothermal Synthesis of  $\alpha$ - and  $\beta$ -MnO<sub>2</sub> Single Crystal Nanowires. *J. Am. Chem. Soc.* **2002**, *124* (12), 2880–1.
- (25) Huo, Y.; Yang, H. Y.; Zhao, X. In *Direct growth of flower-like  $\delta$ -MnO<sub>2</sub> on three-dimensional graphene for high-performance rechargeable Li-O<sub>2</sub> batteries*, ASME Turbo Expo 2008: Power for Land, Sea, and Air, 2008; 2008; pp 1105–1113.
- (26) Wang, F.; Dai, H.; Deng, J.; Bai, G.; Ji, K.; Liu, Y. Manganese oxides with rod-, wire-, tube-, and flower-like morphologies: highly effective catalysts for the removal of toluene. *Environ. Sci. Technol.* **2012**, *46* (7), 4034–4041.
- (27) Cao, Y.; Xiao, L.; Wang, W.; Choi, D.; Nie, Z.; Yu, J.; Saraf, L. V.; Yang, Z.; Liu, J. ChemInform Abstract: Reversible Sodium Ion Insertion in Single Crystalline Manganese Oxide Nanowires with Long Cycle Life. *Adv. Mater.* **2011**, *23* (28), 3155–60.
- (28) Yuan, J.; Li, W. N.; Gomez, S.; Suib, S. L. Shape-controlled synthesis of manganese oxide octahedral molecular sieve three-dimensional nanostructures. *J. Am. Chem. Soc.* **2005**, *127* (41), 14184–5.
- (29) Xu, H.; Qu, Z.; Zhao, S.; Mei, J.; Quan, F.; Yan, N. Different crystal-forms of one-dimensional MnO<sub>2</sub> nanomaterials for the catalytic oxidation and adsorption of elemental mercury. *J. Hazard. Mater.* **2015**, *299*, 86–93.
- (30) Xu, H.; Qu, Z.; Zong, C.; Huang, W.; Quan, F.; Yan, N. MnO<sub>x</sub>/Graphene for the Catalytic Oxidation and Adsorption of Elemental Mercury. *Environ. Sci. Technol.* **2015**, *49* (11), 6823–6830.
- (31) Xu, R.; Xun, W.; Wang, D.; Zhou, K.; Li, Y. Surface structure effects in nanocrystal MnO<sub>2</sub> and Ag/MnO<sub>2</sub> catalytic oxidation of CO. *J. Catal.* **2006**, *237* (2), 426–430.
- (32) Tang, X.; Hao, J.; Yi, H.; Li, J.; Low-temperature, S. C. R. of NO with NH<sub>3</sub> over AC/C supported manganese-based monolithic catalysts. *Catal. Today* **2007**, *126* (3–4), 406–411.
- (33) Wang, L.; Huang, B.; Su, Y.; Zhou, G.; Wang, K.; Luo, H.; Ye, D. Manganese oxides supported on multi-walled carbon nanotubes for selective catalytic reduction of NO with NH<sub>3</sub>: Catalytic activity and characterization. *Chem. Eng. J.* **2012**, *192* (2), 232–241.
- (34) Shen, B.; Wang, Y.; Wang, F.; Liu, T. The effect of Ce–Zr on NH<sub>3</sub>-SCR activity over MnO<sub>x</sub>(0.6)/Ce<sub>0.5</sub>Zr<sub>0.5</sub>O<sub>2</sub> at low temperature. *Chem. Eng. J.* **2014**, *236* (2), 171–180.
- (35) Agüero, F. N.; Scian, A.; Barbero, B. P.; Cadús, L. E. Influence of the Support Treatment on the Behavior of MnO<sub>x</sub>/Al<sub>2</sub>O<sub>3</sub> Catalysts used in VOC Combustion. *Catal. Lett.* **2009**, *128* (3–4), 268–280.
- (36) Tan, H. T.; Chen, Y.; Zhou, C.; Jia, X.; Zhu, J.; Chen, J.; Rui, X.; Yan, Q.; Yang, Y. Palladium nanoparticles supported on manganese oxide–CNT composites for solvent-free aerobic oxidation of alcohols: Tuning the properties of Pd active sites using MnO<sub>x</sub>. *Appl. Catal., B* **2012**, *119–120* (3), 166–174.
- (37) Chen, S.; Zhu, J.; Wu, X.; Han, Q.; Wang, X. Graphene oxide–MnO<sub>2</sub> nanocomposites for supercapacitors. *ACS Nano* **2010**, *4* (5), 2822–30.
- (38) Reddy, A. L.; Shaijumon, M. M.; Gowda, S. R.; Ajayan, P. M. Coaxial MnO<sub>2</sub>/carbon nanotube array electrodes for high-performance lithium batteries. *Nano Lett.* **2009**, *9* (3), 1002–6.

- (39) Xu, M.; Kong, L.; Zhou, W.; Li, H. Hydrothermal synthesis and pseudocapacitance properties of  $\alpha$ -MnO<sub>2</sub> hollow spheres and hollow urchins. *J. Phys. Chem. C* **2007**, *111* (51), 19141–19147.
- (40) Pan, X.; Fan, Z.; Chen, W.; Ding, Y.; Luo, H.; Bao, X. Enhanced ethanol production inside carbon-nanotube reactors containing catalytic particles. *Nat. Mater.* **2007**, *6* (7), 507–11.
- (41) Zhang, J.; Jiang, J.; Zhao, X. S. Synthesis and Capacitive Properties of Manganese Oxide Nanosheets Dispersed on Functionalized Graphene Sheets. *J. Phys. Chem. C* **2011**, *115* (14), 6448–6454.
- (42) Li, J.; Yan, N.; Qu, Z.; Qiao, S.; Yang, S.; Guo, Y.; Liu, P.; Jia, J. Catalytic Oxidation of Elemental Mercury over the Modified Catalyst Mn/ $\alpha$ -Al<sub>2</sub>O<sub>3</sub> at Lower Temperatures. *Environ. Sci. Technol.* **2010**, *44* (1), 426–31.
- (43) Jin, R.; Liu, Y.; Wu, Z.; Wang, H.; Gu, T. Low-temperature selective catalytic reduction of NO with NH<sub>3</sub> over Mn Ce oxides supported on TiO<sub>2</sub> and Al<sub>2</sub>O<sub>3</sub>: A comparative study. *Chemosphere* **2010**, *78* (9), 1160–6.
- (44) Xingyi, W.; Qian, K.; Dao, L. Catalytic combustion of chlorobenzene over MnOx–CeO<sub>2</sub> mixed oxide catalysts. *Appl. Catal., B* **2009**, *86* (3–4), 166–175.
- (45) Yan, N.; Chen, W.; Chen, J.; Qu, Z.; Guo, Y.; Yang, S.; Jia, J. Significance of RuO<sub>2</sub> Modified SCR Catalyst for Elemental Mercury Oxidation in Coal-fired Flue Gas. *Environ. Sci. Technol.* **2011**, *45* (13), 5725–30.
- (46) Ma, L.; Sui, S.; Zhai, Y. Preparation and characterization of Ir/TiC catalyst for oxygen evolution. *J. Power Sources* **2008**, *177* (2), 470–477.
- (47) Bai, B.; Li, J. Positive Effects of K<sup>+</sup> Ions on Three-Dimensional Mesoporous Ag/Co<sub>3</sub>O<sub>4</sub> Catalyst for HCHO Oxidation. *ACS Catal.* **2014**, *4* (8), 2753–2762.
- (48) Jögi, I.; Erme, K.; Laan, A. H. M. Oxidation of nitrogen oxide in hybrid plasma-catalytic reactors based on DBD and Fe<sub>2</sub>O<sub>3</sub>. *Eur. Phys. J. Appl. Phys.* **2013**, *61* (2), 81–86.
- (49) Pan, W. G.; Zhou, Y.; Guo, R. T.; Zhen, W. L.; Hong, J. N.; Xu, H. J.; Jin, Q.; Ding, C. G.; Guo, S. Y. Influence of calcination temperature on CeO<sub>2</sub>-CuO catalyst for the selective catalytic reduction of NO with NH<sub>3</sub>. *Environ. Prog. Sustainable Energy* **2014**, *33* (2), 385–389.
- (50) Peng, Y.; Li, J.; Huang, X.; Li, X.; Su, W.; Sun, X.; Wang, D.; Hao, J. Deactivation mechanism of potassium on the V<sub>2</sub>O<sub>5</sub>/CeO<sub>2</sub> catalysts for SCR reaction: acidity, reducibility and adsorbed-NOx. *Environ. Sci. Technol.* **2014**, *48* (8), 4515–20.
- (51) Zeng, T.; Zhang, X.; Wang, S.; Niu, H.; Cai, Y. Spatial confinement of a Co<sub>3</sub>O<sub>4</sub> catalyst in hollow metal-organic frameworks as a nanoreactor for improved degradation of organic pollutants. *Environ. Sci. Technol.* **2015**, *49* (4), 2350–7.
- (52) Xu, H.; Xie, J.; Ma, Y.; Qu, Z.; Zhao, S.; Chen, W.; Huang, W.; Yan, N. The cooperation of Fe Sn in a MnO<sub>x</sub> complex sorbent used for capturing elemental mercury. *Fuel* **2015**, *140*, 803–809.
- (53) Yang, S.; Xiong, S.; Liao, Y.; Xiao, X.; Qi, F.; Peng, Y.; Fu, Y.; Shan, W.; Li, J. Mechanism of N<sub>2</sub>O formation during the low-temperature selective catalytic reduction of NO with NH<sub>3</sub> over Mn-Fe spinel. *Catal. Sci. Technol.* **2015**, *5* (4), 10354–62.
- (54) Sinquin, G.; Petit, C.; Hindermann, J.; Kiennemann, A. Study of the formation of LaMO<sub>3</sub> (M= Co, Mn) perovskites by propionates precursors: application to the catalytic destruction of chlorinated VOCs. *Catal. Today* **2001**, *70* (1), 183–196.
- (55) Gutiérrez-Ortiz, J. I.; de Rivas, B. D.; López-Fonseca, R.; Martín, S.; González-Velasco, J. R. Structure of Mn–Zr mixed oxides catalysts and their catalytic performance in the gas-phase oxidation of chlorocarbons. *Chemosphere* **2007**, *68* (6), 1004–1012.
- (56) Chang, H.; Li, J.; Chen, X.; Ma, L.; Yang, S.; Schwank, J. W.; Hao, J. Effect of Sn on MnO<sub>x</sub>–CeO<sub>2</sub> catalyst for SCR of NO<sub>x</sub> by ammonia: enhancement of activity and remarkable resistance to SO<sub>2</sub>. *Catal. Commun.* **2012**, *27*, 54–57.
- (57) Liu, C.; Xian, H.; Jiang, Z.; Wang, L.; Zhang, J.; Zheng, L.; Tan, Y.; Li, X. Insight into the improvement effect of the Ce doping into the SnO<sub>2</sub> catalyst for the catalytic combustion of methane. *Appl. Catal., B* **2015**, *176–177*, 542–552.
- (58) Chang, H.; Chen, X.; Li, J.; Ma, L.; Wang, C.; Liu, C.; Schwank, J. W.; Hao, J. Improvement of Activity and SO<sub>2</sub> Tolerance of Sn-Modified MnOx–CeO<sub>2</sub> Catalysts for NH<sub>3</sub>-SCR at Low Temperatures. *Environ. Sci. Technol.* **2013**, *47* (10), 5294–5301.
- (59) Xie, J.; Qu, Z.; Yan, N.; Yang, S.; Chen, W.; Hu, L.; Huang, W.; Liu, P. Novel regenerable sorbent based on Zr-Mn binary metal oxides for flue gas mercury retention and recovery. *J. Hazard. Mater.* **2013**, *261* (20), 206–213.
- (60) Wu, Z.; Jin, R.; Liu, Y.; Wang, H. Ceria modified MnOx/TiO<sub>2</sub> as a superior catalyst for NO reduction with NH<sub>3</sub> at low-temperature. *Catal. Commun.* **2008**, *9* (13), 2217–2220.
- (61) Lee, S. M.; Park, K. H.; Hong, S. C. MnOx/CeO<sub>2</sub>–TiO<sub>2</sub> mixed oxide catalysts for the selective catalytic reduction of NO with NH<sub>3</sub> at low temperature. *Chem. Eng. J.* **2012**, *195–196*, 323–331.
- (62) Lin, F.; Wu, X.; Liu, S.; Weng, D.; Huang, Y. Preparation of MnOx–CeO<sub>2</sub>–Al<sub>2</sub>O<sub>3</sub> mixed oxides for NOx-assisted soot oxidation: Activity, structure and thermal stability. *Chem. Eng. J.* **2013**, *226*, 105–112.
- (63) Zhu, J.; Li, H.; Zhong, L.; Xiao, P.; Xu, X.; Yang, X.; Zhao, Z.; Li, J. Perovskite oxides: preparation, characterizations, and applications in heterogeneous catalysis. *ACS Catal.* **2014**, *4* (9), 2917–2940.
- (64) Keav, S.; Matam, S. K.; Weidenkaff, A.; Ferri, D. Structured Perovskite-Based Catalysts and Their Application as Three-Way Catalytic Converters—A Review. *Catalysts* **2014**, *4* (3), 226–255.
- (65) Mishra, A.; Prasad, R. Preparation and Application of Perovskite Catalysts for Diesel Soot Emissions Control: An Overview. *Catal. Rev.: Sci. Eng.* **2014**, *56* (1), 57–81.
- (66) Liang, Y.; Wang, H.; Zhou, J.; Li, Y.; Wang, J.; Regier, T.; Dai, H. Covalent hybrid of spinel manganese-cobalt oxide and graphene as advanced oxygen reduction electrocatalysts. *J. Am. Chem. Soc.* **2012**, *134* (7), 3517–3523.
- (67) Yang, S.; Guo, Y.; Yan, N.; Wu, D.; He, H.; Xie, J.; Qu, Z.; Yang, C.; Jia, J. A novel multi-functional magnetic Fe-Ti-V spinel catalyst for elemental mercury capture and callback from flue gas. *Chem. Commun.* **2010**, *46* (44), 8377–9.
- (68) Heck, R. M. Catalytic abatement of nitrogen oxides—stationary applications. *Catal. Today* **1999**, *53* (4), 519–523.
- (69) Tayyeb Javed, M.; Irfan, N.; Gibbs, B. M. Control of combustion-generated nitrogen oxides by selective non-catalytic reduction. *J. Environ. Manage.* **2007**, *83* (3), 251–289.
- (70) Apostolescu, N.; Geiger, B.; Hizbullah, K.; Jan, M. T.; Kureti, S.; Reichert, D.; Schott, F.; Weisweiler, W. Selective catalytic reduction of nitrogen oxides by ammonia on iron oxide catalysts. *Appl. Catal., B* **2006**, *62* (1–2), 104–114.
- (71) Zheng, Y.; Jensen, A. D.; Johnsson, J. E. Deactivation of V<sub>2</sub>O<sub>5</sub>-WO<sub>3</sub>-TiO<sub>2</sub> SCR catalyst at a biomass-fired combined heat and power plant. *Appl. Catal., B* **2005**, *60* (3), 253–264.
- (72) Cao, Y.; Gao, Z.; Zhu, J.; Wang, Q.; Huang, Y.; Chiu, C.; Parker, B.; Chu, P.; Pan, W. Impacts of Halogen Additions on Mercury Oxidation, in A Slipstream Selective Catalyst Reduction (SCR), Reactor When Burning Sub-Bituminous Coal. *Environ. Sci. Technol.* **2008**, *42* (1), 256–61.
- (73) Ettireddy, P. R.; Ettireddy, N.; Mamedov, S.; Boolchand, P.; Smirniotis, P. G. Surface characterization studies of TiO<sub>2</sub> supported manganese oxide catalysts for low temperature SCR of NO with NH<sub>3</sub>. *Appl. Catal., B* **2007**, *76* (1–2), 123–134.
- (74) Kim, Y. J.; Kwon, H. J.; Heo, I. S.; Nam, I. S.; Cho, B. K.; Choung, J. W.; Cha, M. S.; Yeo, G. K. Mn–Fe/ZSM5 as a low-temperature SCR catalyst to remove NOx from diesel engine exhaust. *Appl. Catal., B* **2012**, *126* (38), 9–21.
- (75) Kapteijn, F.; Singoredjo, L.; Andreini, A.; Moulijn, J. Activity and selectivity of pure manganese oxides in the selective catalytic reduction of nitric oxide with ammonia. *Appl. Catal., B* **1994**, *3* (2), 173–189.
- (76) Tang, X.; Li, J.; Sun, L.; Hao, J. Origination of N<sub>2</sub>O from NO reduction by NH<sub>3</sub> over  $\beta$ -MnO<sub>2</sub> and  $\alpha$ -Mn<sub>2</sub>O<sub>3</sub>. *Appl. Catal., B* **2010**, *99* (1), 156–162.
- (77) Wang, C.; Sun, L.; Cao, Q.; Hu, B.; Huang, Z.; Tang, X. Surface structure sensitivity of manganese oxides for low-temperature selective

catalytic reduction of NO with NH<sub>3</sub>. *Appl. Catal., B* **2011**, *101* (3), 598–605.

(78) Lin, Q.; Li, J.; Ma, L.; Hao, J. Selective catalytic reduction of NO with NH<sub>3</sub> over Mn–Fe/USY under lean burn conditions. *Catal. Today* **2010**, *151* (3), 251–256.

(79) Qi, G.; Yang, R. T.; Chang, R. Low-temperature SCR of NO with NH<sub>3</sub> over USY-supported manganese oxide-based catalysts. *Catal. Lett.* **2003**, *87* (1–2), 67–71.

(80) Brandenberger, S.; Kröcher, O.; Tissler, A.; Althoff, R. Effect of structural and preparation parameters on the activity and hydrothermal stability of metal-exchanged ZSM-5 in the selective catalytic reduction of NO by NH<sub>3</sub>. *Ind. Eng. Chem. Res.* **2011**, *50* (8), 4308–4319.

(81) Carja, G.; Kameshima, Y.; Okada, K.; Madhusoodana, C. D. Mn–Ce/ZSMS as a new superior catalyst for NO reduction with NH<sub>3</sub>. *Appl. Catal., B* **2007**, *73* (1), 60–64.

(82) Kim, Y. J.; Kwon, H. J.; Heo, I.; Nam, I.-S.; Cho, B. K.; Choung, J. W.; Cha, M.-S.; Yeo, G. K. Mn–Fe/ZSMS as a low-temperature SCR catalyst to remove NO<sub>x</sub> from diesel engine exhaust. *Appl. Catal., B* **2012**, *126*, 9–21.

(83) Liang, X.; Li, J.; Lin, Q.; Sun, K. Synthesis and characterization of mesoporous Mn/Al-SBA-15 and its catalytic activity for NO reduction with ammonia. *Catal. Commun.* **2007**, *8* (12), 1901–1904.

(84) Xie, L.; Liu, F.; Ren, L.; Shi, X.; Xiao, F.-S.; He, H. Excellent Performance of One-Pot Synthesized Cu-SSZ-13 Catalyst for the Selective Catalytic Reduction of NO<sub>x</sub> with NH<sub>3</sub>. *Environ. Sci. Technol.* **2014**, *48* (1), 566–572.

(85) Gao, R.; Zhang, D.; Maitarad, P.; Shi, L.; Rungrotmongkol, T.; Li, H.; Zhang, J.; Cao, W. Morphology-Dependent Properties of MnO<sub>x</sub>/ZrO<sub>2</sub>–CeO<sub>2</sub> Nanostructures for the Selective Catalytic Reduction of NO with NH<sub>3</sub>. *J. Phys. Chem. C* **2013**, *117* (20), 10502–10511.

(86) Marbán, G.; Valdés-Solís, T.; Fuertes, A. B. Mechanism of low-temperature selective catalytic reduction of NO with NH<sub>3</sub> over carbon-supported Mn<sub>3</sub>O<sub>4</sub>: Role of surface NH<sub>3</sub> species: SCR mechanism. *J. Catal.* **2004**, *226* (1), 138–155.

(87) Maitarad, P.; Zhang, D.; Gao, R.; Shi, L.; Li, H.; Huang, L.; Rungrotmongkol, T.; Zhang, J. Combination of Experimental and Theoretical Investigations of MnO<sub>x</sub>/Ce<sub>0.9</sub>Zr<sub>0.1</sub>O<sub>2</sub> Nanorods for Selective Catalytic Reduction of NO with Ammonia. *J. Phys. Chem. C* **2013**, *117* (19), 9999–10006.

(88) Xu, H.; Zhang, Q.; Qiu, C.; Lin, T.; Gong, M.; Chen, Y. Tungsten modified MnO<sub>x</sub>–CeO<sub>2</sub>/ZrO<sub>2</sub> monolith catalysts for selective catalytic reduction of NO<sub>x</sub> with ammonia. *Chem. Eng. Sci.* **2012**, *76*, 120–128.

(89) Zhang, Q.; Qiu, C.; Xu, H.; Lin, T.; Lin, Z.; Gong, M.; Chen, Y. Low-temperature selective catalytic reduction of NO with NH<sub>3</sub> over monolith catalyst of MnO<sub>x</sub>/CeO<sub>2</sub>–ZrO<sub>2</sub>–Al<sub>2</sub>O<sub>3</sub>. *Catal. Today* **2011**, *175* (1), 171–176.

(90) Guan, B.; Lin, H.; Zhu, L.; Huang, Z. Selective Catalytic Reduction of NO<sub>x</sub> with NH<sub>3</sub> over Mn, Ce Substitution Ti<sub>0.9</sub>V<sub>0.1</sub>O<sub>2</sub>– $\delta$  Nanocomposites Catalysts Prepared by Self-Propagating High-Temperature Synthesis Method. *J. Phys. Chem. C* **2011**, *115* (26), 12850–12863.

(91) Liu, Z.; Li, Y.; Zhu, T.; Su, H.; Zhu, J. Selective Catalytic Reduction of NO<sub>x</sub> by NH<sub>3</sub> over Mn-Promoted V<sub>2</sub>O<sub>5</sub>/TiO<sub>2</sub> Catalyst. *Ind. Eng. Chem. Res.* **2014**, *53* (33), 12964–12970.

(92) Jiang, B.; Wu, Z.; Liu, Y.; Lee, S.; Ho, W. DRIFT study of the SO<sub>2</sub> effect on low-temperature SCR reaction over Fe–Mn/TiO<sub>2</sub>. *J. Phys. Chem. C* **2010**, *114* (11), 4961–4965.

(93) Niu, J.; Deng, J.; Liu, W.; Zhang, L.; Wang, G.; Dai, H.; He, H.; Zi, X. Nanosized perovskite-type oxides La<sub>1-x</sub>Sr<sub>x</sub>MO<sub>3- $\delta$</sub>  (M = Co, Mn; x = 0, 0.4) for the catalytic removal of ethylacetate. *Catal. Today* **2007**, *126* (3), 420–429.

(94) Wu, Z.; Jiang, B.; Liu, Y.; Wang, H.; Jin, R. DRIFT study of manganese/titania-based catalysts for low-temperature selective catalytic reduction of NO with NH<sub>3</sub>. *Environ. Sci. Technol.* **2007**, *41* (16), 5812–5817.

(95) Liu, C.; Chen, L.; Li, J.; Ma, L.; Arandiyán, H.; Du, Y.; Xu, J.; Hao, J. Enhancement of activity and sulfur resistance of CeO<sub>2</sub>

supported on TiO<sub>2</sub>–SiO<sub>2</sub> for the selective catalytic reduction of NO by NH<sub>3</sub>. *Environ. Sci. Technol.* **2012**, *46* (11), 6182–6189.

(96) Tang, X.; Hao, J.; Yi, H.; Li, J. Low-temperature SCR of NO with NH<sub>3</sub> over AC/C supported manganese-based monolithic catalysts. *Catal. Today* **2007**, *126* (3), 406–411.

(97) Wang, L.; Huang, B.; Su, Y.; Zhou, G.; Wang, K.; Luo, H.; Ye, D. Manganese oxides supported on multi-walled carbon nanotubes for selective catalytic reduction of NO with NH<sub>3</sub>: Catalytic activity and characterization. *Chem. Eng. J.* **2012**, *192*, 232–241.

(98) Su, Y.; Fan, B.; Wang, L.; Liu, Y.; Huang, B.; Fu, M.; Chen, L.; Ye, D. MnO<sub>x</sub> supported on carbon nanotubes by different methods for the SCR of NO with NH<sub>3</sub>. *Catal. Today* **2013**, *201*, 115–121.

(99) Wang, X.; Zheng, Y.; Lin, J. Highly dispersed Mn–Ce mixed oxides supported on carbon nanotubes for low-temperature NO reduction with NH<sub>3</sub>. *Catal. Commun.* **2013**, *37*, 96–99.

(100) Wang, X.; Zheng, Y.; Xu, Z.; Wang, X.; Chen, X. Amorphous MnO<sub>2</sub> supported on carbon nanotubes as a superior catalyst for low temperature NO reduction with NH<sub>3</sub>. *RSC Adv.* **2013**, *3* (29), 11539–11542.

(101) Wang, Y.; Ge, C.; Zhan, L.; Li, C.; Qiao, W.; Ling, L. MnO<sub>x</sub>–CeO<sub>2</sub>/Activated Carbon Honeycomb Catalyst for Selective Catalytic Reduction of NO with NH<sub>3</sub> at Low Temperatures. *Ind. Eng. Chem. Res.* **2012**, *51* (36), 11667–11673.

(102) Zhang, D.; Zhang, L.; Shi, L.; Fang, C.; Li, H.; Gao, R.; Huang, L.; Zhang, J. In situ supported MnO<sub>x</sub>–CeO<sub>x</sub> on carbon nanotubes for the low-temperature selective catalytic reduction of NO with NH<sub>3</sub>. *Nanoscale* **2013**, *5* (3), 1127–1136.

(103) Smirniotis, P. G.; Sreekanth, P. M.; Peña, D. A.; Jenkins, R. G. Manganese Oxide Catalysts Supported on TiO<sub>2</sub>, Al<sub>2</sub>O<sub>3</sub>, and SiO<sub>2</sub>: A Comparison for Low-Temperature SCR of NO with NH<sub>3</sub>. *Ind. Eng. Chem. Res.* **2006**, *45* (19), 6436–6443.

(104) Qi, G.; Yang, R. T. Performance and kinetics study for low-temperature SCR of NO with NH<sub>3</sub> over MnO<sub>x</sub>–CeO<sub>2</sub> catalyst. *J. Catal.* **2003**, *217* (2), 434–441.

(105) Yang, S.; Liao, Y.; Xiong, S.; Qi, F.; Dang, H.; Xiao, X.; Li, J. N<sub>2</sub> Selectivity of NO Reduction by NH<sub>3</sub> over MnO<sub>x</sub>–CeO<sub>2</sub>: Mechanism and Key Factors. *J. Phys. Chem. C* **2014**, *118* (37), 21500–21508.

(106) Eigenmann, F.; Maciejewski, M.; Baiker, A. Selective reduction of NO by NH<sub>3</sub> over manganese–cerium mixed oxides: Relation between adsorption, redox and catalytic behavior. *Appl. Catal., B* **2006**, *62* (3), 311–318.

(107) Jin, R.; Liu, Y.; Wu, Z.; Wang, H.; Gu, T. Relationship between SO<sub>2</sub> poisoning effects and reaction temperature for selective catalytic reduction of NO over Mn–Ce/TiO<sub>2</sub> catalyst. *Catal. Today* **2010**, *153* (3), 84–89.

(108) Qi, G.; Yang, R. T.; Chang, R. MnO<sub>x</sub>–CeO<sub>2</sub> mixed oxides prepared by co-precipitation for selective catalytic reduction of NO with NH<sub>3</sub> at low temperatures. *Appl. Catal., B* **2004**, *51* (2), 93–106.

(109) Chen, Z.; Wang, F.; Li, H.; Yang, Q.; Wang, L.; Li, X. Low-Temperature Selective Catalytic Reduction of NO<sub>x</sub> with NH<sub>3</sub> over Fe–Mn Mixed-Oxide Catalysts Containing Fe<sub>3</sub>Mn<sub>3</sub>O<sub>8</sub> Phase. *Ind. Eng. Chem. Res.* **2012**, *51* (1), 202–212.

(110) Liu, F.; He, H. Selective catalytic reduction of NO with NH<sub>3</sub> over manganese substituted iron titanate catalyst: reaction mechanism and H<sub>2</sub>O/SO<sub>2</sub> inhibition mechanism study. *Catal. Today* **2010**, *153* (3), 70–76.

(111) Long, R. Q.; Yang, R. T.; Chang, R. Low temperature selective catalytic reduction (SCR) of NO with NH<sub>3</sub> over Fe–Mn based catalysts. *Chem. Commun.* **2002**, *5*, 452–453.

(112) Kang, M.; Park, E. D.; Kim, J. M.; Yie, J. E. Cu–Mn mixed oxides for low temperature NO reduction with NH<sub>3</sub>. *Catal. Today* **2006**, *111* (3), 236–241.

(113) Li, Q.; Yang, H.; Nie, A.; Fan, X.; Zhang, X. Catalytic Reduction of NO with NH<sub>3</sub> over V<sub>2</sub>O<sub>5</sub>–MnO<sub>x</sub>/TiO<sub>2</sub>–Carbon Nanotube Composites. *Catal. Lett.* **2011**, *141* (8), 1237–1242.

(114) Liu, F.; Shan, W.; Lian, Z.; Xie, L.; Yang, W.; He, H. Novel MnWO<sub>x</sub> catalyst with remarkable performance for low temperature NH<sub>3</sub>–SCR of NO<sub>x</sub>. *Catal. Sci. Technol.* **2013**, *3* (10), 2699–2707.

- (115) Thirupathi, B.; Smirniotis, P. G. Nickel-doped Mn/TiO<sub>2</sub> as an efficient catalyst for the low-temperature SCR of NO with NH<sub>3</sub>: Catalytic evaluation and characterizations. *J. Catal.* **2012**, *288*, 74–83.
- (116) Thirupathi, B.; Smirniotis, P. G. Effect of nickel as dopant in Mn/TiO<sub>2</sub> catalysts for the low-temperature selective reduction of NO with NH<sub>3</sub>. *Catal. Lett.* **2011**, *141* (10), 1399–1404.
- (117) Wan, Y.; Zhao, W.; Tang, Y.; Li, L.; Wang, H.; Cui, Y.; Gu, J.; Li, Y.; Shi, J. Ni-Mn bi-metal oxide catalysts for the low temperature SCR removal of NO with NH<sub>3</sub>. *Appl. Catal., B* **2014**, *148-149*, 114–122.
- (118) Zhang, L.; Shi, L.; Huang, L.; Zhang, J.; Gao, R.; Zhang, D. Rational Design of High-Performance DeNO<sub>x</sub> Catalysts Based on Mn x Co<sub>3-x</sub>O<sub>4</sub> Nanocages Derived from Metal–Organic Frameworks. *ACS Catal.* **2014**, *4* (6), 1753–1763.
- (119) Zuo, J.; Chen, Z.; Wang, F.; Yu, Y.; Wang, L.; Li, X. Low-Temperature Selective Catalytic Reduction of NO x with NH<sub>3</sub> over Novel Mn–Zr Mixed Oxide Catalysts. *Ind. Eng. Chem. Res.* **2014**, *53* (7), 2647–2655.
- (120) Cai, S.; Zhang, D.; Zhang, L.; Huang, L.; Li, H.; Gao, R.; Shi, L.; Zhang, J. Comparative study of 3D ordered macroporous Ce<sub>0.75</sub>Zr<sub>0.25</sub>O<sub>2-δ</sub> (M= Fe, Cu, Mn, Co) for selective catalytic reduction of NO with NH<sub>3</sub>. *Catal. Sci. Technol.* **2014**, *4* (1), 93–101.
- (121) Liu, Y.; Gu, T.; Weng, X.; Wang, Y.; Wu, Z.; Wang, H. DRIFT studies on the selectivity promotion mechanism of Ca-modified Ce-Mn/TiO<sub>2</sub> catalysts for low-temperature NO reduction with NH<sub>3</sub>. *J. Phys. Chem. C* **2012**, *116* (31), 16582–16592.
- (122) Liu, Z.; Yi, Y.; Zhang, S.; Zhu, T.; Zhu, J.; Wang, J. Selective catalytic reduction of NO<sub>x</sub> with NH<sub>3</sub> over Mn-Ce mixed oxide catalyst at low temperatures. *Catal. Today* **2013**, *216*, 76–81.
- (123) Liu, Z.; Zhu, J.; Li, J.; Ma, L.; Woo, S. I. Novel Mn–Ce–Ti Mixed-Oxide Catalyst for the Selective Catalytic Reduction of NO x with NH<sub>3</sub>. *ACS Appl. Mater. Interfaces* **2014**, *6* (16), 14500–14508.
- (124) Li, H.; Zhang, D.; Maitarad, P.; Shi, L.; Gao, R.; Zhang, J.; Cao, W. In situ synthesis of 3D flower-like NiMnFe mixed oxides as monolith catalysts for selective catalytic reduction of NO with NH<sub>3</sub>. *Chem. Commun.* **2012**, *48* (86), 10645–10647.
- (125) Li, H.; Zhang, D.; Maitarad, P.; Shi, L.; Gao, R.; Zhang, J.; Cao, W. In situ synthesis of 3D flower-like NiMnFe mixed oxides as monolith catalysts for selective catalytic reduction of NO with NH<sub>3</sub>. *Chem. Commun.* **2012**, *48* (86), 10645–10647.
- (126) Yang, S.; Wang, C.; Chen, J.; Peng, Y.; Ma, L.; Chang, H.; Chen, L.; Liu, C.; Xu, J.; Li, J.; Yan, N. A novel magnetic Fe–Ti–V spinel catalyst for the selective catalytic reduction of NO with NH<sub>3</sub> in a broad temperature range. *Catal. Sci. Technol.* **2012**, *2* (5), 915–917.
- (127) Yang, S.; Wang, C.; Li, J.; Yan, N.; Ma, L.; Chang, H. Low temperature selective catalytic reduction of NO with NH<sub>3</sub> over Mn–Fe spinel: performance, mechanism and kinetic study. *Appl. Catal., B* **2011**, *110*, 71–80.
- (128) Zamudio, M. A.; Russo, N.; Fino, D. Low Temperature NH<sub>3</sub> Selective Catalytic Reduction of NO<sub>x</sub> over Substituted MnCr<sub>2</sub>O<sub>4</sub> Spinel-Oxide Catalysts. *Ind. Eng. Chem. Res.* **2011**, *50* (11), 6668–6672.
- (129) Li, X.; Yin, Y.; Yao, C.; Zuo, S.; Lu, X.; Luo, S.; Ni, C. La<sub>1-x</sub>Ce<sub>x</sub>MnO<sub>3</sub>/attapulgite nanocomposites as catalysts for NO reduction with NH<sub>3</sub> at low temperature. *Particuology* **2016**, *26*, 66–72.
- (130) Duan, J.; Tan, J.; Yang, L.; Wu, S.; Hao, J. Concentration, sources and ozone formation potential of volatile organic compounds (VOCs) during ozone episode in Beijing. *Atmos. Res.* **2008**, *88* (1), 25–35.
- (131) Lathière, J.; Hauglustaine, D. A.; Friend, A. D.; De Noblet-Ducoudré, N.; Viovy, N.; Folberth, G. A. Impact of climate variability and land use changes on global biogenic volatile organic compound emissions. *Atmos. Chem. Phys.* **2006**, *6* (8), 2129–2146.
- (132) Qiao, P.; Xu, S.; Zhang, D.; Li, R.; Zou, S.; Liu, J.; Yi, W.; Li, J.; Fan, J. Sub-10 nm Au-Pt-Pd alloy trimetallic nanoparticles with a high oxidation-resistant property as efficient and durable VOC oxidation catalysts. *Chem. Commun.* **2014**, *50* (79), 11713–6.
- (133) Kim, S. C.; Shim, W. G. Catalytic combustion of VOCs over a series of manganese oxide catalysts. *Appl. Catal., B* **2010**, *98* (3), 180–185.
- (134) Alvarez-Galvan, M.; de la Pena O’Shea, V.; Fierro, J.; Arias, P. Alumina-supported manganese-and manganese–palladium oxide catalysts for VOCs combustion. *Catal. Commun.* **2003**, *4* (5), 223–228.
- (135) Aguilera, D. A.; Perez, A.; Molina, R.; Moreno, S. Cu–Mn and Co–Mn catalysts synthesized from hydrotalcites and their use in the oxidation of VOCs. *Appl. Catal., B* **2011**, *104* (1), 144–150.
- (136) Morales, M. R.; Barbero, B. P.; Cadús, L. E. Total oxidation of ethanol and propane over Mn-Cu mixed oxide catalysts. *Appl. Catal., B* **2006**, *67* (3–4), 229–236.
- (137) Delimaris, D.; Ioannides, T. VOC oxidation over MnO<sub>x</sub>–CeO<sub>2</sub> catalysts prepared by a combustion method. *Appl. Catal., B* **2008**, *84* (1), 303–312.
- (138) Tian, Z.-Y.; Tchoua Ngamou, P. H.; Vannier, V.; Kohse-Höinghaus, K.; Bahlawane, N. Catalytic oxidation of VOCs over mixed Co–Mn oxides. *Appl. Catal., B* **2012**, *117-118*, 125–134.
- (139) Delimaris, D.; Ioannides, T. VOC oxidation over MnO<sub>x</sub>–CeO<sub>2</sub> catalysts prepared by a combustion method. *Appl. Catal., B* **2008**, *84* (1), 303–312.
- (140) Gutiérrez-Ortiz, J. I.; de Rivas, B.; López-Fonseca, R.; Martín, S.; González-Velasco, J. R. Structure of Mn–Zr mixed oxides catalysts and their catalytic performance in the gas-phase oxidation of chlorocarbons. *Chemosphere* **2007**, *68* (6), 1004–1012.
- (141) Azalim, S.; Franco, M.; Brahmī, R.; Giraudon, J.-M.; Lamoniér, J.-F. Removal of oxygenated volatile organic compounds by catalytic oxidation over Zr–Ce–Mn catalysts. *J. Hazard. Mater.* **2011**, *188* (1), 422–427.
- (142) Lu, H.; Zhou, Y.; Huang, H.; Zhang, B.; Chen, Y. In-situ synthesis of monolithic Cu-Mn-Ce/cordierite catalysts towards VOCs combustion. *J. Rare Earths* **2011**, *29* (9), 855–860.
- (143) Spinicci, R.; Faticanti, M.; Marini, P.; De Rossi, S.; Porta, P. Catalytic activity of LaMnO<sub>3</sub> and LaCoO<sub>3</sub> perovskites towards VOCs combustion. *J. Mol. Catal. A: Chem.* **2003**, *197* (1), 147–155.
- (144) Zhang, L.; Wang, S.; Wang, L.; Wu, Y.; Duan, L.; Wu, Q.; Wang, F.; Yang, M.; Yang, H.; Hao, J.; Liu, X. Updated emission inventories for speciated atmospheric mercury from anthropogenic sources in China. *Environ. Sci. Technol.* **2015**, *49* (5), 3185–3194.
- (145) Wang, S.; Zhang, L.; Wang, L.; Wu, Q.; Wang, F.; Hao, J. A review of atmospheric mercury emissions, pollution and control in China. *Front. Environ. Sci. Eng.* **2014**, *8* (5), 631–649.
- (146) Zhang, L.; Wright, L. P.; Blanchard, P. A review of current knowledge concerning dry deposition of atmospheric mercury. *Atmos. Environ.* **2009**, *43* (37), 5853–5864.
- (147) Gao, Y.; Zhang, Z.; Wu, J.; Duan, L.; Umar, A.; Sun, L.; Guo, Z.; Wang, Q. A Critical Review on the Heterogeneous Catalytic Oxidation of Elemental Mercury in Flue Gases. *Environ. Sci. Technol.* **2013**, *47* (19), 10813–23.
- (148) Pavlish, J. H.; Sondreal, E. A.; Mann, M. D.; Olson, E. S.; Galbreath, K. C.; Laudal, D. L.; Benson, S. A. Status review of mercury control options for coal-fired power plants. *Fuel Process. Technol.* **2003**, *82* (2), 89–165.
- (149) Cimino, S.; Scala, F. Removal of elemental mercury by MnO<sub>x</sub> catalysts supported on TiO<sub>2</sub> or Al<sub>2</sub>O<sub>3</sub>. *Ind. Eng. Chem. Res.* **2016**, *55* (18), 5133–5138.
- (150) Li, J.; Yan, N.; Qu, Z.; Qiao, S.; Yang, S.; Guo, Y.; Liu, P.; Jia, J. Catalytic oxidation of elemental mercury over the modified catalyst Mn/α-Al<sub>2</sub>O<sub>3</sub> at lower temperatures. *Environ. Sci. Technol.* **2010**, *44* (1), 426–431.
- (151) Qiao, S.; Chen, J.; Li, J.; Qu, Z.; Liu, P.; Yan, N.; Jia, J. Adsorption and catalytic oxidation of gaseous elemental mercury in flue gas over MnO<sub>x</sub>/alumina. *Ind. Eng. Chem. Res.* **2009**, *48* (7), 3317–3322.
- (152) Xie, J.; Yan, N.; Yang, S.; Qu, Z.; Chen, W.; Zhang, W.; Li, K.; Liu, P.; Jia, J. Synthesis and characterization of nano-sized Mn–TiO<sub>2</sub> catalysts and their application to removal of gaseous elemental mercury. *Res. Chem. Intermed.* **2012**, *38* (9), 2511–2522.

- (153) ZHANG, A.-c.; ZHANG, Z.-h.; SHI, J.-m.; CHEN, G.-y.; ZHOU, C.-s.; SUN, L.-s. Effect of preparation methods on the performance of MnOx-TiO<sub>2</sub> adsorbents for Hg<sup>0</sup> removal and SO<sub>2</sub> resistance. *Journal of Fuel Chemistry and Technology* **2015**, *43* (10), 1258–1266.
- (154) Li, H.; Wu, C.-Y.; Li, Y.; Li, L.; Zhao, Y.; Zhang, J. Role of flue gas components in mercury oxidation over TiO<sub>2</sub> supported MnOx-CeO<sub>2</sub> mixed-oxide at low temperature. *J. Hazard. Mater.* **2012**, *243*, 117–123.
- (155) Mei, Z.; Shen, Z.; Zhao, Q.; Wang, W.; Zhang, Y. Removal and recovery of gas-phase element mercury by metal oxide-loaded activated carbon. *J. Hazard. Mater.* **2008**, *152* (2), 721–729.
- (156) Xing, L.; Xu, Y.; Zhong, Q. Mn and Fe modified fly ash as a superior catalyst for elemental mercury capture under air conditions. *Energy Fuels* **2012**, *26* (8), 4903–4909.
- (157) Zhao, B.; Liu, X.; Zhou, Z.; Shao, H.; Xu, M. Catalytic oxidation of elemental mercury by Mn–Mo/CNT at low temperature. *Chem. Eng. J.* **2016**, *284*, 1233–1241.
- (158) Jampaiah, D.; Ippolito, S. J.; Sabri, Y. M.; Tardio, J.; Selvakannan, P.; Nafady, A.; Reddy, B. M.; Bhargava, S. K. Ceria–zirconia modified MnO<sub>x</sub> catalysts for gaseous elemental mercury oxidation and adsorption. *Catal. Sci. Technol.* **2016**, *6*, 1792–1803.
- (159) Yang, S.; Guo, Y.; Yan, N.; Qu, Z.; Xie, J.; Yang, C.; Jia, J. Capture of gaseous elemental mercury from flue gas using a magnetic and sulfur poisoning resistant sorbent Mn/γ-Fe<sub>2</sub>O<sub>3</sub> at lower temperatures. *J. Hazard. Mater.* **2011**, *186* (1), 508–515.
- (160) Li, H.; Wu, C.-Y.; Li, Y.; Zhang, J. Superior activity of MnOx-CeO<sub>2</sub>/TiO<sub>2</sub> catalyst for catalytic oxidation of elemental mercury at low flue gas temperatures. *Appl. Catal., B* **2012**, *111–112*, 381–388.
- (161) Dang, H.; Liao, Y.; Ng, T. W.; Huang, G.; Xiong, S.; Xiao, X.; Yang, S.; Wong, P. K. The simultaneous centralized control of elemental mercury emission and deep desulfurization from the flue gas using magnetic Mn–Fe spinel as a co-benefit of the wet electrostatic precipitator. *Fuel Process. Technol.* **2016**, *142*, 345–351.
- (162) Yang, S.; Yan, N.; Guo, Y.; Wu, D.; He, H.; Qu, Z.; Li, J.; Zhou, Q.; Jia, J. Gaseous elemental mercury capture from flue gas using magnetic nanosized (Fe<sub>3-x</sub>Mn<sub>x</sub>)<sub>1-δ</sub>O<sub>4</sub>. *Environ. Sci. Technol.* **2011**, *45* (4), 1540–1546.
- (163) Xie, J.; Qu, Z.; Yan, N.; Yang, S.; Chen, W.; Hu, L.; Huang, W.; Liu, P. Novel regenerable sorbent based on Zr–Mn binary metal oxides for flue gas mercury retention and recovery. *J. Hazard. Mater.* **2013**, *261*, 206–213.
- (164) Xie, J.; Xu, H.; Qu, Z.; Huang, W.; Chen, W.; Ma, Y.; Zhao, S.; Liu, P.; Yan, N. Sn–Mn binary metal oxides as non-carbon sorbent for mercury removal in a wide-temperature window. *J. Colloid Interface Sci.* **2014**, *428*, 121–127.
- (165) Xu, H.; Xie, J.; Ma, Y.; Qu, Z.; Zhao, S.; Chen, W.; Huang, W.; Yan, N. The cooperation of Fe Sn in a MnOx complex sorbent used for capturing elemental mercury. *Fuel* **2015**, *140*, 803–809.
- (166) Wang, Y.; Shen, B.; He, C.; Yue, S.; Wang, F. Simultaneous Removal of NO and Hg<sup>0</sup> from Flue Gas over Mn–Ce/Ti-PILCs. *Environ. Sci. Technol.* **2015**, *49* (15), 9355–63.
- (167) Liao, Y.; Xiong, S.; Dang, H.; Xiao, X.; Yang, S.; Wong, P. K. The centralized control of elemental mercury emission from the flue gas by a magnetic regenerable Fe–Ti–Mn spinel. *J. Hazard. Mater.* **2015**, *299*, 740–746.
- (168) Yang, S.; Guo, Y.; Yan, N.; Wu, D.; He, H.; Qu, Z.; Jia, J. Elemental mercury capture from flue gas by magnetic Mn–Fe spinel: effect of chemical heterogeneity. *Ind. Eng. Chem. Res.* **2011**, *50* (16), 9650–9656.
- (169) Xu, H.; Qu, Z.; Zong, C.; Quan, F.; Mei, J.; Yan, N. Catalytic oxidation and adsorption of Hg<sup>0</sup> over low-temperature NH<sub>3</sub>-SCR LaMnO<sub>3</sub> perovskite oxide from flue gas. *Appl. Catal., B* **2016**, *186*, 30–40.
- (170) Stanmore, B. R.; Brillhac, J.-F.; Gilot, P. The oxidation of soot: a review of experiments, mechanisms and models. *Carbon* **2001**, *39* (15), 2247–2268.
- (171) Atribak, I.; Bueno-López, A.; García-García, A.; Navarro, P.; Frías, D.; Montes, M. Catalytic activity for soot combustion of birnessite and cryptomelane. *Appl. Catal., B* **2010**, *93* (3), 267–273.
- (172) Atribak, I.; Bueno-López, A.; García-García, A.; Navarro, P.; Frías, D.; Montes, M. Catalytic activity for soot combustion of birnessite and cryptomelane. *Appl. Catal., B* **2010**, *93* (3–4), 267–273.
- (173) Legutko, P.; Jakubek, T.; Kaspera, W.; Stelmachowski, P.; Sojka, Z.; Kotarba, A. Soot oxidation over K-doped manganese and iron spinels—How potassium precursor nature and doping level change the catalyst activity. *Catal. Commun.* **2014**, *43*, 34–37.
- (174) Wagloehner, S.; Nitzer-Noski, M.; Kureti, S. Oxidation of soot on manganese oxide catalysts. *Chem. Eng. J.* **2015**, *259*, 492–504.
- (175) Li, Q.; Meng, M.; Xian, H.; Tsubaki, N.; Li, X.; Xie, Y.; Hu, T.; Zhang, J. Hydrothermal-Derived Mn<sub>x</sub>Mg<sub>3-x</sub> AlO Catalysts Used for Soot Combustion, NO<sub>x</sub> Storage and Simultaneous Soot-NO<sub>x</sub> Removal. *Environ. Sci. Technol.* **2010**, *44* (12), 4747–4752.
- (176) Sánchez Escribano, V.; Fernández López, E. F.; Gallardo-Amores, J.; del Hoyo Martínez, C.; Pistarino, C.; Panizza, M.; Resini, C.; Busca, G. A study of a ceria–zirconia-supported manganese oxide catalyst for combustion of diesel soot particles. *Combust. Flame* **2008**, *153* (1), 97–104.
- (177) Liu, S.; Wu, X.; Weng, D.; Li, M.; Lee, H.-R. Combined promoting effects of platinum and MnOx–CeO<sub>2</sub> supported on alumina on NO<sub>x</sub>-assisted soot oxidation: Thermal stability and sulfur resistance. *Chem. Eng. J.* **2012**, *203*, 25–35.
- (178) Liang, Q.; Wu, X.; Weng, D.; Xu, H. Oxygen activation on Cu/Mn–Ce mixed oxides and the role in diesel soot oxidation. *Catal. Today* **2008**, *139* (1), 113–118.
- (179) Wang, H.; Liu, J.; Zhao, Z.; Wei, Y.; Xu, C. Comparative study of nanometric Co-, Mn- and Fe-based perovskite-type complex oxide catalysts for the simultaneous elimination of soot and NO<sub>x</sub> from diesel engine exhaust. *Catal. Today* **2012**, *184* (1), 288–300.
- (180) Wu, X.; Lin, F.; Xu, H.; Weng, D. Effects of adsorbed and gaseous NO<sub>x</sub> species on catalytic oxidation of diesel soot with MnOx–CeO<sub>2</sub> mixed oxides. *Appl. Catal., B* **2010**, *96* (1), 101–109.
- (181) Wu, X.; Liu, S.; Lin, F.; Weng, D. Nitrate storage behavior of Ba/MnOx–CeO<sub>2</sub> catalyst and its activity for soot oxidation with heat transfer limitations. *J. Hazard. Mater.* **2010**, *181* (1), 722–728.
- (182) Li, L.; Shen, X.; Wang, P.; Meng, X.; Song, F. Soot capture and combustion for perovskite La–Mn–O based catalysts coated on honeycomb ceramic in practical diesel exhaust. *Appl. Surf. Sci.* **2011**, *257* (22), 9519–9524.
- (183) Teraoka, Y.; Kanada, K.; Kagawa, S. Synthesis of LaKMnO perovskite-type oxides and their catalytic property for simultaneous removal of NO<sub>x</sub> and diesel soot particulates. *Appl. Catal., B* **2001**, *34* (1), 73–78.
- (184) Torres Sanchez, R. M. T.; Ueda, A.; Tanaka, K.; Haruta, M. Selective Oxidation of CO in Hydrogen over Gold Supported on Manganese Oxides. *J. Catal.* **1997**, *168* (1), 125–127.
- (185) Krämer, M.; Schmidt, T.; Stöwe, K.; Müller, F.; Natter, H.; Maier, W. F. Structural and catalytic aspects of sol–gel derived copper manganese oxides as low-temperature CO oxidation catalyst. *Appl. Catal., A* **2006**, *313* (1), 112–112.
- (186) Alonso, L.; Palacios, J. M. Performance and Recovering of a Zn-Doped Manganese Oxide as a Regenerable Sorbent for Hot Coal Gas Desulfurization. *Energy Fuels* **2002**, *16* (6), 1550–1556.
- (187) Gac, W. The influence of silver on the structural, redox and catalytic properties of the cryptomelane-type manganese oxides in the low-temperature CO oxidation reaction. *Appl. Catal., B* **2007**, *75* (1–2), 107–117.
- (188) Guo, Q.; Liu, Y. MnOx modified Co<sub>3</sub>O<sub>4</sub>-CeO<sub>2</sub> catalysts for the preferential oxidation of CO in H<sub>2</sub>-rich gases. *Appl. Catal., B* **2008**, *82* (1–2), 19–26.
- (189) Yasyerli, S. Cerium–manganese mixed oxides for high temperature H<sub>2</sub>S removal and activity comparisons with V–Mn, Zn–Mn, Fe–Mn sorbents. *Chem. Eng. Process.* **2008**, *47* (47), 577–584.